aerospace

MDPI

Article

On the Extrapolation of Stability Derivatives to Combined Changes in Airspeed and Angles of Attack and Sideslip

Luís M. B. C. Campos [1] and Joaquim M. G. Marques [2,*]

[1] CCTAE, IDMEC, Instituto Superior Técnico, Universidade de Lisboa, Av. Rovisco Pais, 1049-001 Lisboa, Portugal; luis.campos@tecnico.ulisboa.pt
[2] CCTAE, IDMEC, Departamento de Engenharia Mecatrónica, Escola de Ciências e Tecnologia, Universidade de Évora, Colégio Luís António Verney, Rua Romão Ramalho, 59, 7000-671 Évora, Portugal
* Correspondence: jmgmarques@uevora.pt

Abstract: The variation in stability derivatives with airspeed and angles of attack and sideslip is determined using only the dependence of the aerodynamic forces and moments on the modulus and direction of the velocity. Analytic extrapolation factors are obtained for all 12 longitudinal plus 12 lateral stability derivatives of linear decoupled motion. The extrapolation factors relate the stability derivatives for two flight conditions with different airspeeds, angles of attack (AoA), and angles of sideslip (AoS). The extrapolation formulas were validated by comparison with results of computational fluid dynamics (CFD) using Reynolds-averaged Navier–Stokes (RANS) equations. The comparison concerns the extrapolated full longitudinal–lateral stability matrix from one landing and one takeoff condition of a V-tailed aircraft, to 10 other landing and takeoff flight cases with different airspeeds, AoAs, and AoSs. Thus, 420 comparisons were made between extrapolated stability derivatives and CFD–RANS results demonstrating the achievable levels of accuracy.

Keywords: aircraft stability; stability derivatives; changes of angles in attack and sideslip and airspeed

Citation: Campos, L.M.B.C.; Marques, J.M.G. On the Extrapolation of Stability Derivatives to Combined Changes in Airspeed and Angles of Attack and Sideslip. *Aerospace* **2022**, *9*, 249. https://doi.org/10.3390/aerospace9050249

Academic Editor: Konstantinos Kontis

Received: 7 December 2021
Accepted: 19 April 2022
Published: 3 May 2022

1. Introduction

The linearization of the equations of motion of a symmetric aircraft lead, in the case of decoupled lateral and longitudinal motion [1–10], to two 4 × 4 matrices each containing 12 nonzero stability derivatives. These stability derivatives can be estimated by four methods: (i) approximate analytical formulas; (ii) empirical numerical corrections; (iii) computational fluid mechanics; (iv) wind tunnel measurements with a model. Besides airspeed, the stability derivatives depend on the angle of attack (AoA) and angle of sideslip (AoS), leading to a matrix of values to be determined, for example, by (v) successive computer runs or (vi) tilting a model in a wind tunnel. A method for estimating the dependency of the stability derivatives on the airspeed, AoA, and AoS can thus reduce the number of computer runs or wind tunnel measurements by extrapolation of results, e.g., between two distinct flight conditions with different airspeeds, AoAs, and AoSs. This kind of extrapolation formula can be used also as a first guess if supported by an estimate of its accuracy.

The starting point is a minimal review of airplane stability (Section 2), starting with the equations of motion of a rigid aircraft (Section 2.1), linearized about a mean state of straight, steady, and level flight (Section 2.2), to identify the 24 non-trivial (that is different from zero and unity) stability derivatives appearing in the decoupled longitudinal and lateral stability matrices (Section 2.3). The dependences on airspeed, AoA, and AoS (Section 3) are considered for the 24 stability derivatives in five sets of 2 + 6 + 6 + 9 + 1, each set with a distinct extrapolation factor relating flight conditions with different airspeeds, AoAs, and AoSs. The five extrapolation factors that apply to all 24 stability derivatives involve only three dimensionless coefficients comparing two flight conditions (Section 3.1). The extrapolation factors are based on approximate quantitative reasoning on how each set of

stability derivatives depends on airspeed, AoA, and AoS (Section 3.2). This leads to a total of five cases, that is, five different extrapolation factors (Section 3.3), involving some or all three dimensionless coefficients (Section 3.1), each applying to a distinct subset of the complete set of 24 stability derivatives.

The extrapolation of stability derivatives is illustrated for a V-tailed single-aisle jetliner design but can be applied not only to V-tailed aircraft [11–15] but to other configurations [16–19], such as blended-wing bodies [20–39] and joined wings [40,41], that can have large number of control surfaces changing their geometry. The effort of determination of each stability derivative for a given airspeed could be reduced from one full table (combinations of the AoA and AoS) to (a) a list (dependence on one extrapolated to the other) or (b) a single value (extrapolation from given AoA and AoS). The extrapolation method also accounts for airspeed changes, leading, together with AoA and AoS, to a parallelepiped of values of each stability derivative, extending the matrix of values for different AoAs and AoSs to a third dimension of different airspeeds. The extrapolation method can be extended to the cross-coupling derivatives between longitudinal and lateral stability that may be nonzero for asymmetric aircraft; also the method of extrapolation factors includes airspeed changes as well as changes in AoA and AoS.

The airspeed, AoA, and AoS are included in the readily measured real time flight data from aerodynamic probes or other sensors of platforms [42,43]. The airspeed, AoA, and AoS can also be obtained by methods that are model independent [44]. Both sources of information on airspeed, AoA, and AoS allow estimation of effects on stability derivatives. The extrapolation factors for the stability derivatives are specified by very simple analytical formulas that can be subject to validation (Section 4) by comparison with well-established methods of CFD, in this case RANS computations. The full longitudinal plus lateral stability matrices are considered for one takeoff and one landing configuration, and then each is extrapolated to 10 distinct landing and takeoff flight cases with different airspeeds, AoAs, and AoSs (Section 4.1). The two sets of 10 extrapolated stability matrices are then compared with the CFD–RANS calculations for the same flight conditions (Section 4.2). This demonstrates the relative accuracy of the extrapolation method versus CFD–RANS for a total of 420 stability derivatives (Section 4.3). The accuracies vary widely from four coincident digits to outliers, showing as a conclusion (Section 5) that the extrapolation method can give some promising results but also leaves plenty of scope for improvement in other cases.

2. Identification of 24 Linear Stability Derivatives

The equations of motion of a rigid symmetric airplane (Section 2.1) are linearized around a mean state of uniform straight and level flight (Section 2.2) to identify the 24 stability derivatives appearing in the decoupled longitudinal and lateral stability matrices (Section 2.3).

2.1. Equations of Motion of a Rigid Airplane

The force balance:

$$\dot{\vec{P}} + \vec{\Omega} \wedge \vec{P} = m\vec{g} + \vec{F} \tag{1}$$

and the moment balance:

$$\dot{\vec{Q}} + \vec{\Omega} \wedge \vec{Q} = \vec{G} \tag{2}$$

involve (i) the weight due to the acceleration of gravity:

$$\vec{g} = g[-\sin\theta, \cos\theta \sin\varphi, \cos\theta \cos\varphi] \tag{3}$$

where θ is the pitch attitude and φ the bank angle; (ii) the aerodynamic (and propulsive) forces (4a) and moments (4b):

$$\vec{F} = [X, Y, Z] \tag{4a}$$

$$\vec{G} = [L, M, N] \tag{4b}$$

in body axis; (iii) the angular velocity vector:

$$\vec{\Omega} = [p, q, r] = [\dot{\varphi} - \dot{\psi}\sin\theta, \dot{\theta}\cos\psi + \dot{\psi}\cos\theta\sin\psi, -\dot{\theta}\sin\psi + \dot{\psi}\cos\theta\cos\psi] \tag{5}$$

where ψ is the track or sideslip angle; (iv) the linear momentum, equal to mass times linear velocity:

$$\vec{P} = m\vec{V} = m[u, v, w] \tag{6}$$

(v) the inertia tensor I_{ij} or radii of gyration R_{ij}:

$$I_{ij} = \begin{bmatrix} I_{xx} & 0 & I_{xz} \\ 0 & I_{yy} & 0 \\ I_{xz} & 0 & I_{zz} \end{bmatrix} = m \begin{bmatrix} R_x^2 & 0 & R_{xz}^2 \\ 0 & R_y^2 & 0 \\ R_{xz}^2 & 0 & R_z^2 \end{bmatrix} \tag{7}$$

which, for an aircraft with a longitudinal symmetry plane, appears in the angular momentum:

$$Q_i = I_{ij}\Omega_j = \left[I_{xx}p + I_{xz}r, I_{yy}q, I_{xz}p + I_{zz}r\right] \tag{8}$$

All these equations have been known since Euler.

The equations of motion in body axis are obtained by substituting (3,4a,6) in the force balance (1):

$$m\left(\dot{u} + qw - rv\right) = -mg\sin\theta + X \tag{9a}$$

$$m\left(\dot{v} + ru - pw\right) = mg\cos\theta\sin\varphi + Y \tag{9b}$$

$$m\left(\dot{w} + pv - qu\right) = mg\cos\theta\cos\varphi + Z \tag{9c}$$

and substituting (4b,8) in the moment balance (2):

$$I_{xx}\dot{p} + I_{xz}\dot{r} + \left(I_{zz} - I_{yy}\right)qr + I_{xz}pq = L \tag{10a}$$

$$I_{yy}\dot{q} + (I_{xx} - I_{zz})pr + I_{xz}\left(r^2 - p^2\right) = M \tag{10b}$$

$$I_{zz}\dot{r} + I_{xz}\dot{p} + \left(I_{yy} - I_{xx}\right)pq - I_{xz}qr = N \tag{10c}$$

Equations (9a–c) and (10b) specify the time derivatives $\dot{u}$, $\dot{v}$, $\dot{w}$, and $\dot{q}$ in terms of other quantities; the time derivatives $\dot{p}$ and $\dot{r}$ are coupled in (10a,c) and may be decoupled:

$$\left(I_{xx} - I_{xz}^2/I_{zz}\right)\dot{p} = L - \left(I_{zz} - I_{yy}\right)qr - I_{xz}pq - \left(I_{xz}/I_{zz}\right)\left[N - \left(I_{yy} - I_{xx}\right)pq + I_{xz}qr\right] \tag{11a}$$

$$\left(I_{zz} - I_{xz}^2/I_{xx}\right)\dot{r} = N - \left(I_{yy} - I_{xx}\right)pq + I_{xz}qr - \left(I_{xz}/I_{xx}\right)\left[L - \left(I_{zz} - I_{yy}\right)qr - I_{xz}pq\right]. \tag{11b}$$

The three force balance (9a–c), three moment balance (10b; 11a,b), and three kinetic conditions (5) after inversion specify $\left(\dot{u}, \dot{v}, \dot{w}, \dot{p}, \dot{q}, \dot{r}, \dot{\theta}, \dot{\psi}, \dot{\varphi}\right)$ as nonlinear functions of (u,v,w,p,q,θ,ψ,φ).

2.2. Linearization about Uniform Straight and Level Flight

For uniform straight and level flight, only the longitudinal velocity u_0 and pitch attitude θ_0 are nonzero:

$$u_0 \neq 0 = v_0 = w_0 = p_0 = q_0 = r_0 = \psi_0 = \varphi_0 = 0 \neq \theta_0 \tag{12}$$

The linearized equations of motion are: (i) force balance (9a–c):

$$m\dot{u} = -mg\cos\theta_0\,\theta + \{X\} \tag{13a}$$

$$m\dot{v} = -mu_0 r + mg\cos\theta_0\,\varphi + \{Y\} \tag{13b}$$

$$m\dot{w} = mu_0 q - mg\sin\theta_0\,\theta + \{Z\} \tag{13c}$$

where the curly brackets { ... } denote linearization of the aerodynamic forces; (ii) moment balance (11a,10b,11c):

$$\left(I_{xx} - I_{xz}^2/I_{zz}\right)\dot{p} = \{L\} - (I_{xz}/I_{zz})\{N\} \tag{14a}$$

$$I_{yy}\dot{q} = \{M\} \tag{14b}$$

$$\left(I_{zz} - I_{xz}^2/I_{xx}\right)\dot{r} = \{N\} - (I_{xz}/I_{xx})\{L\} \tag{14c}$$

(iii) the kinematic conditions (5):

$$\dot{\theta} = q \tag{15a}$$

$$\dot{\psi}\cos\theta_0 = r \tag{15b}$$

$$\dot{\varphi} = p. \tag{15c}$$

This completes the specification of all 9 derivatives $\left(\dot{u}, \dot{v}, \dot{w}, \dot{p}, \dot{q}, \dot{r}, \dot{\theta}, \dot{\psi}, \dot{\varphi}\right)$.

In order to write explicitly (13a–c); (14a–c), it is necessary to linearize the aerodynamic forces:

$$[X, Y, Z] = \frac{1}{2}\rho S\Big\{\ (u_0 + u)^2 + v^2 + w^2\Big\}[C_X, C_Y, C_Z] \tag{16}$$

and moments:

$$[L, M, N] = \frac{1}{2}\rho Sc\Big\{(u_0 + u)^2 + v^2 + w^2\Big\}[C_L, C_M, C_N] \tag{17}$$

in body axis, e.g.:

$$\begin{array}{l}\{X\} = \frac{1}{2}\rho S\{u_0(2uC_X + u_0 C_{Xu}) \\ +u_0^2\left(vC_{Xv} + wC_{Xw} + pC_{Xp} + qC_{Xq} + rC_{Xr} + \theta C_{X\theta} + \psi C_{X\psi}\right) + u_0^2\left(\delta_a C_{X\delta_a} + \delta_r C_{X\delta_r} + \delta_l C_{X\delta_l}\right)\}\end{array} \tag{18}$$

and likewise for (*Y*,*Z*,*L*,*M*,*N*), wherein are included aileron δ_a and right δ_r and left δ_l tail deflections.

2.3. Decoupled Longitudinal and Lateral Stability Matrices

Substituting (18) and analogue relations for (*Y*,*Z*,*L*,*M*,*N*) in (13a–c); (14a–c), using (15a–c), and assuming longitudinal–lateral decoupling leads to two sets of four autonomous differential equations involving the longitudinal stability matrix:

$$\begin{bmatrix} \frac{2m}{\rho Su_0^2}\dot{u} \\ \frac{2m}{\rho Su_0^2}\dot{w} \\ \frac{2mR_y^2}{\rho Scu_0^2}\dot{q} \\ \dot{\theta} \end{bmatrix} = \begin{bmatrix} C_{Xu} + \frac{2}{u_0}C_X & C_{Xw} & C_{Xq} & C_{X\theta} - \frac{2mg\cos\theta_0}{\rho Su_0^2} \\ C_{Zu} + \frac{2}{u_0}C_Z & C_{Zw} & C_{Zq} - \frac{2m}{\rho Su_0} & C_{Z\theta} - \frac{2mg\sin\theta_0}{\rho Su_0^2} \\ C_{Mu} + \frac{2}{u_0}C_M & C_{Mw} & C_{Mq} & C_{M\theta} \\ 0 & 0 & 1 & 0 \end{bmatrix} \begin{bmatrix} u \\ w \\ q \\ \theta \end{bmatrix} \tag{19}$$

and the lateral stability matrix:

$$\begin{bmatrix} \frac{2m}{\rho S u_0^2}\dot{\bar{v}} \\ \frac{2m\left(R_x^2 - R_{xz}^4/R_z^2\right)}{\rho S c u_0^2}\dot{p} \\ \frac{2m\left(R_z^2 - R_{xz}^4/R_x^2\right)}{\rho S c u_0^3}\dot{r} \\ \dot{\psi} \end{bmatrix} = \begin{bmatrix} C_{Yu} + \frac{2}{u_0}C_Y & C_{Yp} & C_{Yr} - \frac{2m}{\rho S u_0} & C_{Y\psi} \\ C_{Lu} + \frac{2}{u_0}C_L - \frac{I_{xz}}{I_{zz}}\left(C_{Nu} + \frac{2}{u_0}C_N\right) & C_{Lp} - \frac{I_{xz}}{I_{zz}}C_{Np} & C_{Lr} - \frac{I_{xz}}{I_{zz}}C_{Nr} & C_{L\psi} - \frac{I_{xz}}{I_{zz}}C_{N\psi} \\ C_{Nu} + \frac{2}{u_0}C_N - \frac{I_{xz}}{I_{zz}}\left(C_{Lu} + \frac{2}{u_0}C_L\right) & C_{Np} - \frac{I_{xz}}{I_{zz}}C_{Lp} & C_{Nr} - \frac{I_{xz}}{I_{zz}}C_{Lr} & C_{N\psi} - \frac{I_{xz}}{I_{zz}}C_{L\psi} \\ 0 & 0 & \sec\theta_0 & 0 \end{bmatrix} \begin{bmatrix} v \\ p \\ r \\ \psi \end{bmatrix} \tag{20}$$

where $\dot{\bar{v}} \equiv \dot{v} - g\cos\theta_0\varphi$. The two sets of autonomous differential Equations (19) and (20) can be rewritten using dimensionless variables (21) and (22), where the r.h.s. is the autonomous vector, containing the rates of change with time of aircraft variables, with the multiplying factors, involving mean state quantities, appearing as factors with the dimensions of inverse time multiplying the dimensionless longitudinal stability matrix:

$$\begin{bmatrix} \frac{\dot{u}}{u_0} \\ \frac{\dot{w}}{u_0} \\ \frac{\dot{q}c}{u_0} \\ \dot{\theta} \end{bmatrix} = \begin{matrix} \frac{\rho S u_0}{2m} \\ \frac{\rho S u_0}{2m} \\ \frac{\rho S c^2 u_0}{2mR_y^2} \\ 1 \end{matrix} \times \begin{bmatrix} C_{Xu} + 2\,C_X & C_{Xw} & C_{Xq} & C_{X\theta} - \frac{2mg\,\cos\theta_0}{\rho S u_0^2} \\ C_{Zu} + 2\,C_Z & C_{Zw} & C_{Zq} - \frac{2m}{\rho S c_0} & C_{Z\theta} - \frac{2mg\,\sin\theta_0}{\rho S u_0^2} \\ C_{Mu} + 2\,C_M & C_{Mw} & C_{Mq} & C_{M\theta} \\ 0 & 0 & 1 & 0 \end{bmatrix} \tag{21}$$

and the dimensionless lateral stability matrix:

$$\begin{bmatrix} \frac{\dot{\bar{v}}}{u_0} \\ \frac{\dot{p}c}{u_0} \\ \frac{\dot{r}c}{u_0} \\ \dot{\psi} \end{bmatrix} = \begin{matrix} \frac{\rho S u_0}{2m} \\ \frac{\rho S c^2 u_0}{2m\left(R_x^2 - \frac{R_{xz}^4}{R_z^2}\right)} \\ \frac{\rho S c^2 u_0}{2m\left(R_x^2 - \frac{R_{xz}^4}{R_z^2}\right)} \\ 1 \end{matrix} \times \begin{bmatrix} C_{Yv} & C_{Yp} & C_{Yr} - \frac{2m}{\rho S c_0} & C_{Y\psi} \\ C_{Lv} - \frac{I_{xz}}{I_{zz}}C_{Nv} & C_{Lp} - \frac{I_{xz}}{I_{zz}}C_{Np} & C_{Lr} - \frac{I_{xz}}{I_{zz}}C_{Nr} & C_{L\psi} - \frac{I_{xz}}{I_{zz}}C_{N\psi} \\ C_{Nv} - \frac{I_{xz}}{I_{zx}}C_{Lv} & C_{Np} - \frac{I_{xz}}{I_{zz}}C_{Lp} & C_{Nr} - \frac{I_{xz}}{I_{zz}}C_{Lr} & C_{N\psi} - \frac{I_{xz}}{I_{zz}}C_{L\psi} \\ 0 & 1 & 0 & 0 \end{bmatrix} \begin{bmatrix} \frac{v}{u_0} \\ \frac{pc}{u_0} \\ \frac{rc}{u_0} \\ \psi \end{bmatrix}. \tag{22}$$

The dimensionless longitudinal (21) and lateral (22) stability matrices involve 24 stability derivatives, whose dependence on airspeed, AoA, and AoS is considered next (Section 3).

3. Extrapolation among Different Airspeeds, AoAs, and AoSs

The extrapolation factors relate the stability derivatives for two flight conditions, with different airspeeds, AoAs, and AoSs, specified by three ratios that act as dimensionless coefficients (Section 3.1). Some or all coefficients appear in five distinct extrapolation factors (Section 3.2), each applying to a distinct subset of the complete set of 24 stability derivatives (Section 3.3).

3.1. Three Coefficients Comparing Two Flight Conditions

The stability derivatives are usually calculated at zero AoA and zero AoS or for nonzero reference values. For generality, the stability derivatives are herein compared between two flight conditions, "1" and "2", with different AoAs, AoSs, and airspeeds (23a) in terms of the ratio of cosines (23b) of AoA, ratio of cosines (23c) of AoS, and ratio (23d) of airspeeds:

$$\{\alpha_1, \beta_1, V_1\} \leftrightarrow \{\alpha_2, \beta_2, V_2\}: \tag{23a}$$

$$A \equiv \frac{\cos\alpha_1}{\cos\alpha_2} \tag{23b}$$

$$B \equiv \frac{\cos\beta_1}{\cos\beta_2} \tag{23c}$$

$$U \equiv \frac{V_1}{V_2} \tag{23d}$$

A set of extrapolation factors for moderate changes in AoA (23b), AoS (23c), and airspeed (23d) is obtained next that applies differently to distinct sets of stability derivatives, e.g., with regard to AoA, AoS, or linear velocities or with regard to angular velocities. This leads to a set of five extrapolation factors covering all 24 stability derivatives, and allowing extrapolation from one flight condition to others.

There are, in the case of a symmetric aircraft with decoupled lateral–longitudinal motion, 32 stability derivatives in two 4×4 stability matrices (21) and (22). Since eight are known from the last lines of (21) and (22), only 24 stability derivatives need to be determined. Of these, 9 are derivatives with regard to angular velocities:

$$f_0 : \left\{ C_{Xq}, C_{Zq}, C_{Mq}; C_{Yp}, C_{Lp}, C_{Np}; C_{Yr}, C_{Lr}, C_{Nr} \right\} . \tag{24}$$

If these are calculated at zero AoA ($\alpha = 0$) and AoS ($\beta = 0$) and airspeed V_0, the correction factor for moderate AoA ($\alpha \neq 0$) and AoS ($\beta \neq 0$) and airspeed V is:

$$f_1 = V \cos\alpha \ \cos\beta \tag{25}$$

All components of the aerodynamic forces (4a) and moments (4b) are proportional to the square of the airspeed, leading to the factor (26):

$$f_2 = (f_1)^2 = V^2 \cos^2\alpha \ \cos^2\beta. \tag{26}$$

The starting point (26) is perhaps the main simplifying assumption in the derivation of extrapolation factors for stability derivatives. It reflects the fact that the main dependence of aerodynamic forces and moments is on the square of the airspeed for the potential flow of an inviscid fluid [45,46]. This is modified by the dependence on airspeed of the Reynolds number for viscous flow [47,48] and the Mach number for high speed flow [49,50]. There is a trade-off between the range of physical flow phenomena that can be accounted for and the simplicity of the extrapolation factors for stability derivatives. The derivatives with regard to the angular velocities (5) imply division by the airspeed, so (26) is divided by f_1, leading back to (27) $\equiv$ (25):

$$f_3 \equiv \frac{f_2}{f_1} = f_1 = V \cos\alpha \cos\beta. \tag{27}$$

The dimensionless stability derivatives (19,20) involve division by the square of the velocity, leading to (28):

$$f_4 \equiv \frac{f_3}{f_1^2} = \frac{1}{f_1} = \frac{1}{V \cos\alpha \cos\beta}, \tag{28}$$

that is, the inverse of (25) $\equiv$ (27). Thus the ratio of (28) is taken for 2 over 1 in the two flight conditions (23a) leading to:

$$f_0 \equiv \frac{f_{42}}{f_{41}} = \frac{f_1}{f_2}, \tag{29}$$

that implies:

$$f_0 = \frac{V_1 \cos\alpha_1 \cos\beta_1}{V_2 \cos\alpha_2 \cos\beta_2} = UAB. \tag{30}$$

This specifies the extrapolation factor (30) for the nine stability derivatives with regard to angular velocities (24), which equals (30) the product of three factors (23b–d). The

example of the analytical expression (30) for the first extrapolation factor, applying to 9 stability derivatives (24), is extended to a further four extrapolation factors applying to the remaining 15 non-trivial stability derivatives (Section 3.2) that is those different from zero and one in (21) and (22).

3.2. Analytical Expressions for the Five Extrapolation Factors

Next are considered the nine stability derivatives with regard to pitch angle and velocities in the vertical plane:

$$f_\alpha : \{C_{X\theta}, C_{Z\theta}, C_{M\theta}; C_{Xu}, C_{Zu}, C_{Mu};\ C_{Xw}, C_{Zw}, C_{Mw}\} \equiv C_{\Phi\alpha}, \tag{31}$$

noting that derivatives with regard to pitch angle $\partial/\partial\theta$ equal derivatives with regard to AoA $\partial/\partial\theta = \partial/\partial\alpha$, because the two angles differ by a constant $\theta - \alpha = \text{const}$. The preceding reasoning applies only up to (26). For example, $C_{\Phi\alpha}$ changes to (32):

$$\frac{\partial}{\partial\theta}(f_2 C_\Phi) = \frac{\partial}{\partial\alpha}\left(C_\Phi\ V^2 \cos^2\alpha\ \cos^2\beta\right) = V^2\cos^2\beta\left[C_{\Phi\alpha}\cos^2\alpha - 2\,C_\Phi\cos\alpha\ \sin\alpha\right]. \tag{32}$$

In (32) is made the further approximation (33):

$$C_\Phi (C_{\Phi\alpha})^{-1} \equiv C_\Phi (\partial C_\Phi/\partial\alpha)^{-1}\ \sim\ \alpha\ \sim \sin\alpha, \tag{33}$$

leading to (34):

$$\frac{\partial}{\partial\theta}(f_2 C_\Phi) = C_{\Phi\alpha}\ V^2\cos^2\beta\left[\cos^2\alpha - 2\ \cos\alpha\ \sin^2\alpha\right] = C_{\Phi\alpha} f_5, \tag{34}$$

with factor (35):

$$f_5 = V^2\cos^2\beta\cos\alpha\left[\cos\alpha - 2\sin^2\alpha\right]. \tag{35}$$

For small AoA (36a), the second term in curved brackets (36b) is much smaller than the first:

$$\alpha^2 << 1/2: \tag{36a}$$

$$2\sin^2\alpha << 1\ \sim \cos\alpha, \tag{36b}$$

and (35) simplifies to (37):

$$f_6 = V^2\cos\alpha\ \cos^2\beta. \tag{37}$$

This factor applies in particular to the stability derivative (38) for the vertical force, which is orthogonal to the horizontal velocity, and the ratio for flight conditions 1 and 2 as in (30) leads to the extrapolation factor (38):

$$C_{Zu} : f_w \equiv \frac{f_{61}}{f_{62}} = \left(\frac{V_1}{V_2}\frac{\cos\beta_1}{\cos\beta_2}\right)^2 \frac{\cos\alpha_1}{\cos\alpha_2} = U^2 A B^2 = f_0\ U\ B, \tag{38}$$

which involves (38) the three factors (23b–d) and is related to (30) by (38). Besides the extrapolation factors (30) and (38) applying to the stability derivatives (24) and (38), respectively, three more distinct extrapolation factors are needed for the remaining 14 stability derivatives (Section 3.3).

3.3. Five Subsets of 24 Extrapolated Stability Derivatives

For the remaining stability derivatives in (31), other than (38), the division of (37) by the square of the airspeed (26) leads to (39):

$$f_7 \equiv \frac{f_6}{f_2} = \frac{1}{\cos\alpha}; \tag{39}$$

the ratio of flight conditions 2 to 1 leads to the extrapolation factor (40):

$$f_\alpha \equiv \frac{f_{72}}{f_{71}} = \frac{\cos\alpha_1}{\cos\alpha_2} \equiv A, \tag{40}$$

which coincides with the factor (40) ≡ (23c) and applies to the stability derivatives (41):

$$f_\alpha : \{C_{X\theta}, C_{Z\theta}, C_{M\theta}; C_{Xw}, C_{Zw}, C_{Mw}\}, \tag{41}$$

that is, (31) except (38), and also except (42):

$$f_u : \{C_{Xu}, C_{Mu}\}. \tag{42}$$

For the latter two stability derivatives (42), the dependence should be on the inverse of airspeed (43a), leading to the extrapolation factor (43b):

$$f_8 = \frac{1}{V} : \tag{43a}$$

$$f_u \equiv \frac{f_{82}}{f_{81}} = \frac{V_1}{V_2} \equiv U \tag{43b}$$

which coincides with (43b) ≡ (23d).

To complete the full set of 24 stability derivatives, there remain to be considered the 6 stability derivatives with regard to the AoS and lateral velocity:

$$f_\beta : \{C_{Y\psi}, C_{L\psi}, C_{N\psi}; C_{Yv}, C_{Lv}, C_{Nv}\} \equiv C_{\Phi\beta}\ ; \tag{44}$$

the lateral forces and associated moments are modified (45) as the projection on the AoS of the airspeed squared:

$$f_9 = \frac{V^2 - v^2}{V^2} = 1 - \sin^2\beta = \cos^2\beta, \tag{45}$$

leading to the extrapolation factor (46):

$$f_\beta \equiv \frac{f_{92}}{f_{91}} = \left(\frac{\cos\beta_2}{\cos\beta_1}\right)^2 \equiv \frac{1}{B^2}, \tag{46}$$

which is related (46) to the ratio (23c) and applies to the stability derivatives (44). Thus, the extrapolation factor (46) for lateral stability derivatives (44) involves only the AoS, whereas the extrapolation factor (40) for longitudinal stability derivatives (41) involves only to AoA. Among the remaining extrapolation factors, there are three cases: (i) the extrapolation factor (43b) for the stability derivatives (42) involves only the ratio of airspeeds (23d); (ii)/(iii) whereas the extrapolation factors (30) and (38), for the stability derivatives (24) and (38), respectively, involve all three ratios (23b–d). The Table 1 indicates the extrapolation factors for all 24 stability derivatives in the five groups that appear in the complete longitudinal plus lateral stability matrix in Table 2.

Table 1. Extrapolation factors for stability derivatives comparing flight conditions 1 (V_1, α_1, β_1) and 2 (V_2, α_2, β_2). Ratios: $U \equiv \frac{V_1}{V_2}$, $A \equiv \frac{\cos\alpha_1}{\cos\alpha_2}$, $B \equiv \frac{\cos\beta_1}{\cos\beta_2}$.

Group	Applies to Stability Derivatives	With Extrapolation Factor
I	C_{Xu}, C_{Mu}	$f_u \equiv U$
II	$C_{Xw}, C_{Zw}, C_{Mw}, C_{X\theta}, C_{Z\theta}, C_{M\theta}$	$f_\alpha \equiv A$
III	$C_{Yv}, C_{Lv}, C_{Nv}, C_{Y\psi}, C_{L\psi}, C_{N\psi}$	$f_\beta \equiv \frac{1}{B^2}$
IV	$C_{Xq}, C_{Zq}, C_{Mq}, C_{Yp}, C_{Lp}, C_{Np}, C_{Yr}, C_{Lr}, C_{Nr}$	$f_0 \equiv UAB$
V	C_{Zu}	$f_w \equiv f_0 UB$

Table 2. Extrapolation factors for stability matrices.

Variable	u/u_0	w/u_0	q (rad/s)	θ (rad)	v/u_0	p (rad/s)	r (rad/s)	φ (rad)
$\dot{u}/u_0$ (s^{-1})	$C_{Xu} \times f_u$	$C_{Xw} \times f_\alpha$	$C_{Xq} \times f_0$	$C_{X\theta} \times f_\alpha$	0	0	0	0
$\dot{w}/u_0$ (s^{-1})	$C_{Zu} \times f_w$	$C_{Zw} \times f_\alpha$	$C_{Zq} \times f_0$	$C_{Z\theta} \times f_\alpha$	0	0	0	0
$\dot{q}$ (rad/s^2)	$C_{Mu} \times f_u$	$C_{Mw} \times f_\alpha$	$C_{Mq} \times f_0$	$C_{M\theta} \times f_\alpha$	0	0	0	0
$\dot{\theta}$ (rad/s)	0	0	1	0	0	0	0	0
$\dot{v}/u_0$ (s^{-1})	0	0	0	0	$C_{Yv} \times f_\beta$	$C_{Yp} \times f_0$	$C_{Yr} \times f_0$	$C_{Y\psi} \times f_\beta$
$\dot{p}$ (rad/s^2)	0	0	0	0	$C_{Lv} \times f_\beta$	$C_{Lp} \times f_0$	$C_{Lr} \times f_0$	$C_{L\psi} \times f_\beta$
$\dot{r}$ (rad/s^2)	0	0	0	0	$C_{Nv} \times f_\beta$	$C_{Np} \times f_0$	$C_{Nr} \times f_0$	$C_{N\psi} \times f_\beta$
$\dot{\varphi}$ (rad/s)	0	0	0	0	0	1	0	0

4. Comparison of Extrapolation with CFD–RANS Data

The extrapolation of stability derivatives is validated by comparison with CFD–RANS data (Section 4.2). The baseline is a landing (takeoff) flight condition 1 (12) with extrapolation to 10 other flight conditions 2 to 11 (13 to 22) with different AoAs, AoSs, and airspeeds (Section 4.1). The comparison with CFD–RANS data for the 10 takeoff and 10 landing matrices indicates the expected accuracy, or otherwise, of all stability derivatives (Section 4.3).

4.1. Extrapolation for Takeoff and Landing Conditions

The extrapolation factors for each element (Table 1) of the stability matrix (Table 2) are used with additional simplifications:

$$\{C_{Xu} + 2C_X, C_{Zu} + 2C_Z, C_{Mu} + 2C_M\} \to \{C_{Xu}, C_{Zu}, C_{Mu}\} \to \{f_u, f_w, f_u\}, \tag{47}$$

$$\left\{C_{Zq} - \frac{2m}{\rho S c_0}, C_{X\theta} - \frac{2mg\cos\theta_0}{\rho S u_0^2}, C_{Z\theta} - \frac{2mg\sin\theta_0}{\rho S u_0^2}\right\} \to \{C_{Zq}, C_{X\theta}, C_{Z\theta}\} \to \{f_0, f_\alpha, f_\alpha\}, \tag{48}$$

$$\left\{C_{Lv} - \frac{I_{xz}}{I_{zz}}C_{Nv}, C_{Nv} - \frac{I_{xz}}{I_{zx}}C_{Lv}, C_{L\psi} - \frac{I_{xz}}{I_{zz}}C_{N\psi}, C_{N\psi} - \frac{I_{xz}}{I_{zz}}C_{L\psi}\right\} \to \{C_{Lv}, C_{Nv}, C_{L\psi}, C_{N\psi}\} \to f_\beta, \tag{49}$$

$$\left\{C_{Lp} - \frac{I_{xz}}{I_{zz}}C_{Np}, C_{Np} - \frac{I_{xz}}{I_{zz}}C_{Lp}, C_{Lr} - \frac{I_{xz}}{I_{zz}}C_{Nr}, C_{Nr} - \frac{I_{xz}}{I_{zz}}C_{Lr}\right\} \to \{C_{Lp}, C_{Np}, C_{Lr}, C_{Nr}\} \to f_0. \tag{50}$$

The additional simplifications (47; 48; 49; 50) are by no means necessary; they could be entirely dispensed with and are made only to simplify the presentation that follows.

The present method of extrapolation of stability derivatives is validated by comparison with direct calculation of stability derivatives by CFD–RANS methods. The chosen aircraft configuration is a V-tailed jet airliner (Figure 1) whose basic characteristics are shown in Table 3. This aircraft design was extensively studied in the research project mentioned in the acknowledgements section [51,52], which aimed at comparing conventional and V-tail designs from several points of view, including aerodynamics, control, and loads. Wind tunnel models were built and tested to validate an extensive CFD database using RANS methods. Although the CFD data may be questionable in a few specific cases, they should mostly provide a baseline for comparison with the extrapolation of stability derivatives in the sense that the deviations between the two sets of data may indicate the expected accuracy of the extrapolation method.

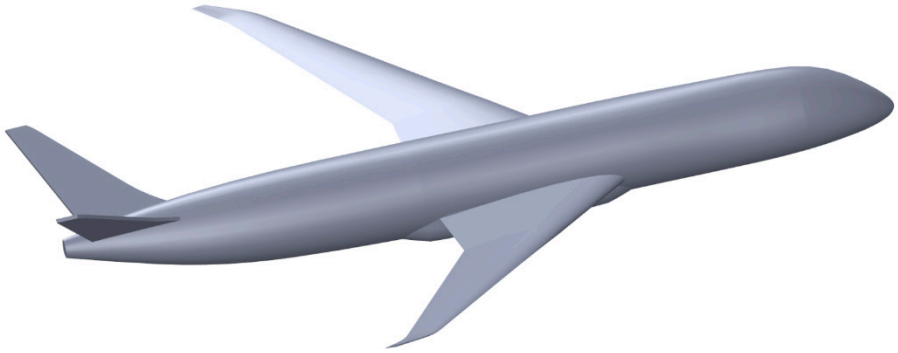

Figure 1. V-tailed single-aisle jet airliner.

Table 3. V-tailed jet airliner basic data.

Variable	Value
wing area	S = 92.00 m^2
mean aerodynamic chord (m.a.c.)	c = 3.545 m
operating mass	m = 30,000 kg
moments of inertia	I_{xx} = 3.159 × 10^5 kg.m^2 I_{yy} = 8.896 × 10^5 kg.m^2 I_{zz} = 1.1473 × 10^6 kg.m^2 I_{xz} = 46,710.6 kg.m^2
c.g. position divided by m.a.c.	x_{cg} = 20.000

The aircraft is considered for 22 flight conditions, 1–11 for landing at high thrust and 12–22 for takeoff with noise cut back, as listed in Table 4. The landing (takeoff) flight condition 1 (12) is taken as the baseline for extrapolation to flight conditions 2 to 11 (13 to 22) with different airspeeds, AoAs, and AoSs. Tables 5 and 6 for landing (takeoff) shows, for each flight condition, (i)–(iii) the total airspeed (51a), AoA (51b), and AoS (51c):

$$V = \left|u^2 + v^2 + w^2\right|^{1/2}, \tag{51a}$$

$$\tan\alpha = \frac{w}{u}, \tag{51b}$$

$$\sin\beta = \frac{v}{V}; \tag{51c}$$

(iv)–(vi) the ratio of airspeeds (23d) and ratios of cosines of AoA (23b) and AoS (23c) between each flight condition 2–11 (13–22) and baseline flight condition 1 (12); (vii)–(viii) the five extrapolation factors (40/30/38/43b) for the stability derivatives (42/41/24/38/42), respectively. Tables 7 and 8 gives the stability matrix for the reference landing (takeoff) flight condition 1 (12) in Table 4, for which the airspeed, AoA, and AoS are repeated at the bottom of Tables 5 and 6.

Tables 9–18 (Tables 19–28), for the landing (takeoff) case, indicate the stability matrices computed by CFD–RANS for each of the flight conditions 2 to 11 (13 to 22) in Tables 4 and 5 (Tables 4 and 6). In brackets appear the extrapolated stability derivatives obtained by applying to flight condition 1 (12) and the stability matrix in Tables 7 and 8. The extrapolation factors were taken from Tables 5 and 6 for the relevant flight condition using the formulas in Table 1 for the stability matrix elements in Table 2. The CFD–RANS computations versus the extrapolated full stability matrices for landing (takeoff) in Tables 9–28 provide 21 comparisons each of CFD–RANS results with extrapolated stability derivatives for a total of 20 × 21 = 420 validations, the accuracy of which is assessed next (Section 4.2).

Table 4. V-tailed jet airliner flight conditions.

Flight Condition	Case	Mass $\times 10^3$ kg	c.g. % m.a.c.	Altitude $\times 10^3$ ft	Airspeed (m/s)		
					u_0	v_0	w_0
Landing with high thrust	1	30.000	20.000	2.000	55.2018	—	7.4411
	2	"	35.000	"	"	—	6.7050
	3	"	50.000	"	"	—	5.9880
	4	37.000	20.000	"	61.3047	—	8.2638
	5	"	35.000	"	61.4093	—	7.4463
	6	"	"	"	61.4299	—	7.2742
	7	"	50.000	"	61.5006	—	6.6500
	8	40.280	20.000	0.000	62.1070	—	8.3719
	9	"	35.000	2.000	64.0735	—	7.7693
	10	"	50.000	"	64.1687	—	0.9385
	11	37.000	20.000	4.000	59.2855	−16.2992	6.7909
Takeoff with cut-back noise	12	30.000	20.000	2.000	57.5070	—	6.6151
	13	"	35.000	"	57.5073	—	6.0399
	14	"	50.000	"	57.6270	—	5.4729
	15	37.000	20.000	"	63.7700	—	8.0950
	16	"	35.000	"	63.8567	—	7.4165
	17	"	"	"	63.6838	—	8.7775
	18	"	50.000	"	63.9306	—	6.7495
	19	43.250	20.000	"	68.8900	—	9.1820
	20	"	35.000	"	68.9913	—	8.4240
	21	"	50.000	"	69.0781	—	7.6797
	22	37.000	35.000	"	81.5830	−16.4993	8.2451

Table 5. Extrapolation from one to ten landing flight conditions.

Flight Condition (Case)	Airspeed V_2 m.s^{-1}	AoA α_2 °	AoS β_2 °	$U \equiv \frac{V_1}{V_2} = f_u$	$A \equiv \frac{\cos\alpha_1}{\cos\alpha_2} = f_\alpha$	$B \equiv \frac{\cos\beta_1}{\cos\beta_2}$	$f_0 \equiv UAB$	$f_w \equiv f_0 UB$	$f_\beta \equiv \frac{1}{B^2}$
2	55.6075	6.9254	0.0000	1.00168	0.99832	1.00000	1.00000	1.00168	1.00000
3	55.5256	6.1909	0.0000	1.00316	0.99685	1.00000	1.00000	1.00316	1.00000
4	61.8592	7.6771	0.0000	0.90045	1.00000	1.00000	0.90045	0.81081	1.00000
5	61.8591	6.9138	0.0000	0.90045	0.99830	1.00000	0.89892	0.80943	1.00000
6	61.8591	6.7532	0.0000	0.90045	0.99796	1.00000	0.89861	0.80916	1.00000
7	61.8591	6.1714	0.0000	0.90045	0.99681	1.00000	0.89758	0.80822	1.00000
8	62.6687	7.6771	0.0000	0.88882	1.00000	1.00000	0.88882	0.79000	1.00000
9	64.5428	6.9137	0.0000	0.86301	0.99830	1.00000	0.86154	0.74352	1.00000
10	64.1756	0.8379	0.0000	0.86795	0.99114	1.00000	0.86026	0.74666	1.00000
11	61.8591	6.5345	−15.2772	0.90045	0.99752	1.03663	0.93112	0.86914	0.93057

(reference flight condition 1: $V_1 = 55.7011$ m.s^{-1}; $\alpha_1 = 7.6771°$; $\beta_1 = 0.0000°$).

Table 6. Extrapolation from one to ten takeoff flight conditions.

Flight Condition (Case)	Airspeed V_2 m.s^{-1}	AoA α_2 °	AoS β_2 °	$U \equiv \frac{V_1}{V_2} = f_u$	$A \equiv \frac{\cos\alpha_1}{\cos\alpha_2} = f_\alpha$	$B \equiv \frac{\cos\beta_1}{\cos\beta_2}$	$f_0 \equiv UAB$	$f_w \equiv f_0 UB$	$f_\beta \equiv \frac{1}{B^2}$
13	57.8236	5.9957	0.0000	1.00108	0.99891	1.00000	0.99999	1.00108	1.00000
14	57.8863	5.4252	0.0000	1.00000	0.99792	1.00000	0.99792	0.99792	1.00000
15	64.2817	7.2345	0.0000	0.90051	1.00142	1.00000	0.90179	0.81207	1.00000
16	64.2859	6.6248	0.0000	0.90045	1.00013	1.00000	0.90056	0.81091	1.00000
17	64.2859	7.8476	0.0000	0.90045	1.00284	1.00000	0.90301	0.81311	1.00000
18	64.2859	6.0267	0.0000	0.90045	0.99897	1.00000	0.89952	0.80997	1.00000
19	69.4992	7.5919	0.0000	0.83290	1.00223	1.00000	0.83477	0.69528	1.00000
20	69.5037	6.9615	0.0000	0.83285	1.00083	1.00000	0.83354	0.69421	1.00000
21	69.5037	6.3438	0.0000	0.83285	0.99957	1.00000	0.83249	0.69334	1.00000
22	83.6421	5.7709	−11.3768	0.69207	0.99851	1.02004	0.70489	0.49761	0.96109

(reference flight condition 12: $V_1 = 57.8862$ m.s^{-1}; $\alpha_1 = 6.5620°$; $\beta_1 = 0.0000°$).

Table 7. Baseline 8 × 8 stability matrix for flight condition 1 in Tables 4 and 5 (reference landing case).

Variable	u/u_0	w/u_0	q (rad/s)	θ (rad)	v/u_0	p (rad/s)	r (rad/s)	φ (rad)
$\dot{u}/u_0$ (s^{-1})	−0.0400	0.1632	−0.0079	−0.3278	0	0	0	0
$\dot{w}/u_0$ (s^{-1})	−0.1899	−0.5865	0.9723	0.0092	0	0	0	0
$\dot{q}$ (rad/s^2)	−0.0218	−1.2966	−0.6409	0	0	0	0	0
$\dot{\theta}$ (rad/s)	0	0	1	0	0	0	0	0
$\dot{v}/u_0$ (s^{-1})	0	0	0	0	−0.1099	0.1280	−0.9822	0.1755
$\dot{p}$ (rad/s^2)	0	0	0	0	−3.2109	−1.7980	1.3652	0
$\dot{r}$ (rad/s^2)	0	0	0	0	0.3203	−0.1977	−0.2076	0
$\dot{\varphi}$ (rad/s)	0	0	0	0	0	1	0	0

Table 8. Baseline 8 × 8 stability matrix for flight condition 12 in Table 4.

Variable	u/u_0	w/u_0	q (rad/s)	θ (rad)	v/u_0	p (rad/s)	r (rad/s)	φ (rad)
$\dot{u}/u_0$ (s^{-1})	−0.0392	0.1544	−0.0069	−0.3113	0	0	0	0
$\dot{w}/u_0$ (s^{-1})	−0.1593	−0.5949	0.9719	0	0	0	0	0
$\dot{q}$ (rad/s^2)	−0.1471	−1.3668	−0.6861	0	0	0	0	0
$\dot{\theta}$ (rad/s)	0	0	1	0	0	0	0	0
$\dot{v}/u_0$ (s^{-1})	0	0	0	0	−0.1152	0.1084	−0.9848	0.1532
$\dot{p}$ (rad/s^2)	0	0	0	0	−3.4457	−1.8621	1.2302	0
$\dot{r}$ (rad/s^2)	0	0	0	0	0.3820	−0.1830	−0.2215	0
$\dot{\varphi}$ (rad/s)	0	0	0	0	0	1	0	0

Table 9. CFD–RANS (extrapolated) 8 × 8 stability matrix for flight condition 2 in Tables 4 and 5 (reference landing case).

Variable	u/u_0	w/u_0	q (rad/s)	θ (rad)	v/u_0	p (rad/s)	r (rad/s)	φ (rad)
$\dot{u}/u_0$ (s^{-1})	−0.0401 (−0.0401)	0.1633 (0.1629)	−0.0063 (−0.0079)	−0.3278 (−0.3272)	0	0	0	0
$\dot{w}/u_0$ (s^{-1})	−0.1901 (−0.1902)	−0.5865 (−0.5855)	0.9781 (0.9723)	0.0092 (0.0092)	0	0	0	0
$\dot{q}$ (rad/s^2)	−0.0218 (−0.0218)	−0.7611 (−1.2944)	−0.6070 (−0.6409)	0	0	0	0	0
$\dot{\theta}$ (rad/s)	0	0	1	0	0	0	0	0
$\dot{v}/u_0$ (s^{-1})	0	0	0	0	−0.1103 (−0.1099)	0.1146 (0.1280)	−0.9849 (−0.9822)	0.1756 (0.1755)
$\dot{p}$ (rad/s^2)	0	0	0	0	−3.2024 (−3.2109)	−1.7946 (−1.7980)	1.2840 (1.3652)	0
$\dot{r}$ (rad/s^2)	0	0	0	0	0.2572 (0.3203)	−0.1868 (−0.1977)	−0.2043 (−0.2076)	0
$\dot{\varphi}$ (rad/s)	0	0	0	0	0	1.0	0	0

Table 10. CFD–RANS (extrapolated) 8 × 8 stability matrix for flight condition 3 in Tables 4 and 5.

Variable	u/u_0	w/u_0	q (rad/s)	θ (rad)	v/u_0	p (rad/s)	r (rad/s)	φ (rad)
$\dot{u}/u_0$ (s^{-1})	−0.0401 (−0.0401)	0.1635 (0.1627)	−0.0046 (−0.0079)	−0.3278 (−0.3268)	0	0	0	0
$\dot{w}/u_0$ (s^{-1})	−0.1902 (−0.1905)	−0.5865 (−0.5847)	0.9838 (0.9723)	0.0092 (0.0092)	0	0	0	0
$\dot{q}$ (rad/s^2)	−0.0218 (−0.0219)	−0.2248 (−1.2925)	−0.5832 (−0.6409)	0	0	0	0	0
$\dot{\theta}$ (rad/s)	0	0	1	0	0	0	0	0
$\dot{v}/u_0$ (s^{-1})	0	0	0	0	−0.1107 (−0.1099)	0.1015 (0.1280)	−0.9874 (−0.9822)	0.1758 (0.1755)
$\dot{p}$ (rad/s^2)	0	0	0	0	−3.1948 (−3.2109)	−1.7913 (−1.7980)	1.2043 (1.3652)	0
$\dot{r}$ (rad/s^2)	0	0	0	0	0.1931 (0.3203)	−0.1767 (−0.1977)	−0.2020 (−0.2076)	0
$\dot{\varphi}$ (rad/s)	0	0	0	0	0	1	0	0

Table 11. CFD–RANS (extrapolated) 8 × 8 stability matrix for flight condition 4 in Tables 4 and 5.

Variable	u/u_0	w/u_0	q (rad/s)	θ (rad)	v/u_0	p (rad/s)	r (rad/s)	φ (rad)
$\dot{u}/u_0$ (s^{-1})	−0.0362 (−0.0360)	0.1644 (0.1632)	−0.0075 (−0.0071)	−0.3290 (−0.3278)	0	0	0	0
$\dot{w}/u_0$ (s^{-1})	−0.1540 (−0.1540)	−0.5281 (−0.5865)	0.9775 (0.8755)	0 (0.0092)	0	0	0	0
$\dot{q}$ (rad/s^2)	−0.0198 (−0.0196)	−1.2966 (−1.2966)	−0.5775 (−0.5771)	0	0	0	0	0
$\dot{\theta}$ (rad/s)	0	0	1	0	0	0	0	0
$\dot{v}/u_0$ (s^{-1})	0	0	0	0	−0.0990 (−0.1099)	0.1291 (0.1153)	−0.9838 (−0.8844)	0.1580 (0.1755)
$\dot{p}$ (rad/s^2)	0	0	0	0	−3.2172 (−3.2109)	−1.6090 (−1.6190)	1.2342 (1.2293)	0
$\dot{r}$ (rad/s^2)	0	0	0	0	0.3570 (0.3203)	−0.1588 (−0.1798)	−0.2009 (−0.1869)	0
$\dot{\varphi}$ (rad/s)	0	0	0	0	0	1	0	0

Table 12. CFD–RANS (extrapolated) 8 × 8 stability matrix for flight condition 5 in Tables 4 and 5.

Variable	u/u_0	w/u_0	q (rad/s)	θ (rad)	v/u_0	p (rad/s)	r (rad/s)	φ (rad)
$\dot{u}/u_0$ (s^{-1})	−0.0362 (−0.0360)	0.1645 (−0.1629)	−0.0056 (−0.0071)	−0.3290 (−0.3272)	0	0	0	0
$\dot{w}/u_0$ (s^{-1})	−0.1541 (−0.1537)	−0.5281 (−0.5855)	0.9822 (0.8740)	0 (0.0092)	0	0	0	0
$\dot{q}$ (rad/s^2)	−0.0198 (−0.0196)	−0.7611 (1.2944)	−0.5465 (−0.5761)	0	0	0	0	0
$\dot{\theta}$ (rad/s)	0	0	1	0	0	0	0	0
$\dot{v}/u_0$ (s^{-1})	0	0	0	0	−0.0993 (−0.1099)	0.1157 (0.1151)	−0.9864 (−0.8829)	0.1582 (0.1755)
$\dot{p}$ (rad/s^2)	0	0	0	0	−3.2063 (−3.2109)	−1.6063 (−1.6163)	1.1611 (1.2272)	0
$\dot{r}$ (rad/s^2)	0	0	0	0	0.2940 (0.3203)	−0.1491 (−0.1777)	−0.1970 (−0.1866)	0
$\dot{\varphi}$ (rad/s)	0	0	0	0	0	1	0	0

Table 13. CFD–RANS (extrapolated) 8 × 8 stability matrix for flight condition 6 in Tables 4 and 5.

Variable	u/u_0	w/u_0	q (rad/s)	θ (rad)	v/u_0	p (rad/s)	r (rad/s)	φ (rad)
$\dot{u}/u_0$ (s^{-1})	−0.0376 (−0.0360)	0.1638 (0.1629)	−0.0056 (−0.0071)	−0.3294 (−0.3271)	0	0	0	0
$\dot{w}/u_0$ (s^{-1})	−0.1533 (−0.1537)	−0.5280 (−0.5853)	0.9822 (0.8737)	0 (0.0092)	0	0	0	0
$\dot{q}$ (rad/s^2)	−0.0377 (−0.0196)	−0.7637 (−1.2940)	−0.5482 (−0.5759)	0	0	0	0	0
$\dot{\theta}$ (rad/s)	0	0	1	0	0	0	0	0
$\dot{v}/u_0$ (s^{-1})	0	0	0	0	−0.0994 (−0.1094) (−0.1099)	0.1129 (0.1150)	−0.9867 (−0.8826)	0.1574 (0.1755)
$\dot{p}$ (rad/s^2)	0	0	0	0	−3.2014 (−3.2109)	−1.6065 (−1.6157)	1.1514 (1.2268)	0
$\dot{r}$ (rad/s^2)	0	0	0	0	0.2965 (0.3203)	−0.1464 (−0.1777)	−0.1977 (−0.1866)	0
$\dot{\varphi}$ (rad/s)	0	0	0	0	0	1	0	0

Table 14. CFD–RANS (extrapolated) 8 × 8 stability matrix for flight condition 7 in Tables 4 and 5.

Variable	u/u_0	w/u_0	q (rad/s)	θ (rad)	v/u_0	p (rad/s)	r (rad/s)	φ (rad)
$\dot{u}/u_0$ (s^{-1})	−0.0363 (−0.0360)	0.1646 (0.1627)	−0.0042 (−0.0071)	−0.3290 (−0.3268)	0	0	0	0
$\dot{w}/u_0$ (s^{-1})	−0.1542 (−0.1545)	−0.5282 (−0.5846)	0.9869 (0.8755)	0 (0.0092)	0	0	0	0
$\dot{q}$ (rad/s^2)	−0.0199 (−0.0196)	−0.2248 (−1.2925)	−0.5252 (−0.5771)	0	0	0	0	0
$\dot{\theta}$ (rad/s)	0	0	1	0	0	0	0	0
$\dot{v}/u_0$ (s^{-1})	0	0	0	0	−0.0997 (−0.1099)	0.1026 (0.1153)	−0.9887 (−0.8844)	0.1583 (0.1755)
$\dot{p}$ (rad/s^2)	0	0	0	0	−3.1962 (−3.2109)	−1.6037 (−1.6190)	1.0894 (1.2254)	0
$\dot{r}$ (rad/s^2)	0	0	0	0	0.2299 (0.3203)	−0.1401 (−0.1780)	−0.1941 (−0.1869)	0
$\dot{\varphi}$ (rad/s)	0	0	0	0	0	1	0	0

Table 15. CFD–RANS (extrapolated) 8 × 8 stability matrix for flight condition 8 in Tables 4 and 5.

Variable	u/u_0	w/u_0	q (rad/s)	θ (rad)	v/u_0	p (rad/s)	r (rad/s)	φ (rad)
$\dot{u}/u_0$ (s^{-1})	−0.0358 (−0.0356)	0.1694 (0.1632)	−0.0072 (−0.0070)	−0.3389 (−0.3278)	0	0	0	0
$\dot{w}/u_0$ (s^{-1})	−0.1457 (−0.1500)	−0.5213 (−0.5865)	0.9781 (0.8642)	0 (0.0092)	0	0	0	0
$\dot{q}$ (rad/s^2)	−0.0191 (−0.0194)	−1.2966 (−1.2966)	−0.5696 (−0.5696)	0	0	0	0	0
$\dot{\theta}$ (rad/s)	0	0	1	0	0	0	0	0
$\dot{v}/u_0$ (s^{-1})	0	0	0	0	−0.0977 (−0.1099)	0.1292 (0.1138)	−0.9840 (−0.8730)	0.1560 (0.1755)
$\dot{p}$ (rad/s^2)	0	0	0	0	−3.2201 (−3.2109)	−1.5851 (−1.5981)	1.2202 (1.2134)	0
$\dot{r}$ (rad/s^2)	0	0	0	0	0.3698 (0.3203)	−0.1502 (−0.1757)	−0.2031 (−0.1845)	0
$\dot{\varphi}$ (rad/s)	0	0	0	0	0	1	0	0

Table 16. CFD–RANS (extrapolated) 8 × 8 stability matrix for flight condition 9 in Tables 4 and 5.

Variable	u/u_0	w/u_0	q (rad/s)	θ (rad)	v/u_0	p (rad/s)	r (rad/s)	φ (rad)
$\dot{u}/u_0$ (s^{-1})	−0.0348 (−0.0345)	0.1650 (0.1629)	−0.0054 (−0.0068)	−0.3295 (−0.3272)	0	0	0	0
$\dot{w}/u_0$ (s^{-1})	−0.1415 (−0.1412)	−0.5002 (−0.5855)	0.9837 (0.8377)	0 (0.0092)	0	0	0	0
$\dot{q}$ (rad/s^2)	−0.0191 (−0.0188)	−0.7611 (−1.2944)	−0.5238 (−0.5522)	0	0	0	0	0
$\dot{\theta}$ (rad/s)	0	0	1	0	0	0	0	0
$\dot{v}/u_0$ (s^{-1})	0	0	0	0	−0.0952 (−0.1099)	0.1161 (0.1103)	−0.9869 (−0.8462)	0.1516 (0.1755)
$\dot{p}$ (rad/s^2)	0	0	0	0	−3.2083 (−3.2109)	−1.5366 (−1.5490)	1.1147 (1.1762)	0
$\dot{r}$ (rad/s^2)	0	0	0	0	0.3068 (0.3203)	−0.1366 (−0.1703)	−0.1932 (−0.1789)	0
$\dot{\varphi}$ (rad/s)	0	0	0	0	0	1	0	0

Table 17. CFD–RANS (extrapolated) 8 × 8 stability matrix for flight condition 10 in Tables 4 and 5.

Variable	u/u_0	w/u_0	q (rad/s)	θ (rad)	v/u_0	p (rad/s)	r (rad/s)	φ (rad)
$\dot{u}/u_0$ (s^{-1})	−0.0348 (−0.0347)	0.1652 (0.1618)	−0.0040 (−0.0068)	−0.3295 (−0.3249)	0	0	0	0
$\dot{w}/u_0$ (s^{-1})	−0.1417 (−0.1418)	−0.5062 (−0.5813)	0.9880 (0.8364)	0 (0.0091)	0	0	0	0
$\dot{q}$ (rad/s^2)	−0.9191 (−0.0189)	−0.2248 (−1.2851)	−0.5033 (−0.5513)	0	0	0	0	0
$\dot{\theta}$ (rad/s)	0	0	1	0	0	0	0	0
$\dot{v}/u_0$ (s^{-1})	0	0	0	0	−0.0955 (−0.1099)	0.1030 (0.1101)	−0.9891 (−0.8450)	0.1517 (0.1755)
$\dot{p}$ (rad/s^2)	0	0	0	0	−3.1973 (−3.2109)	−1.5342 (−1.5468)	1.0460 (1.1744)	0
$\dot{r}$ (rad/s^2)	0	0	0	0	0.2427 (0.3203)	−0.1279 (−0.1701)	−0.1902 (−0.1786)	0
$\dot{\varphi}$ (rad/s)	0	0	0	0	0	1	0	0

Table 18. CFD–RANS (extrapolated) 8 × 8 stability matrix for flight condition 11 in Tables 4 and 5.

Variable	u/u_0	w/u_0	q (rad/s)	θ (rad)	v/u_0	p (rad/s)	r (rad/s)	φ (rad)
$\dot{u}/u_0$ (s^{-1})	−0.0459 (−0.0360)	0.1602 (0.1628)	−0.0054 (−0.0074)	−0.3190 (−0.3270)	0	0	0	0
$\dot{w}/u_0$ (s^{-1})	−0.1573 (−0.1650)	−0.5471 (−0.5850)	0.9815 (0.9053)	0 (0.0092)	0	0	0	0
$\dot{q}$ (rad/s^2)	−0.0477 (−0.0196)	−0.7641 (−1.2934)	−0.5482 (−0.5968)	0	0	0	0	0
$\dot{\theta}$ (rad/s)	0	0	1	0	0	0	0	0
$\dot{v}/u_0$ (s^{-1})	0	0	0	0	−0.0960 (−0.1023)	0.1092 (0.1192)	−0.9874 (−0.9145)	0.1509 (0.1633)
$\dot{p}$ (rad/s^2)	0	0	0	0	−3.1950 (−2.9880)	−1.6047 (−1.6742)	1.1382 (1.2712)	0
$\dot{r}$ (rad/s^2)	0	0	0	0	0.2983 (0.2981)	−0.1429 (−0.1840)	−0.1983 (−0.1933)	0
$\dot{\varphi}$ (rad/s)	0	0	0	0	0	1	0	0

Table 19. CFD–RANS (extrapolated) 8 × 8 stability matrix for flight condition 13 in Tables 4 and 22 (reference takeoff case).

Variable	u/u_0	w/u_0	q (rad/s)	θ (rad)	v/u_0	p (rad/s)	r (rad/s)	φ (rad)
(s^{-1})	−0.0394 (−0.0392)	0.1551 (0.1542)	−0.0055 (−0.0069)	−0.3113 (−0.3110)	0	0	0	0
$\dot{w}/u_0$ (s^{-1})	−0.1601 (−0.1595)	−0.5950 (−0.5943)	0.9777 (0.9719)	0	0	0	0	0
$\dot{q}$ (rad/s^2)	−0.1471 (−0.1473)	−0.7907 (−1.3653)	−0.6472 (−0.6861)	0	0	0	0	0
$\dot{\theta}$ (rad/s)	0	0	1	0	0	0	0	0
$\dot{v}/u_0$ (s^{-1})	0	0	0	0	−0.1158 (−0.1152)	0.0983 (0.1084)	−0.9869 (−0.9848)	0.1539 (0.1532)
$\dot{p}$ (rad/s^2)	0	0	0	0	−3.4318 (−3.4457)	−1.8597 (−1.8621)	1.1589 (1.2302)	0
$\dot{r}$ (rad/s^2)	0	0	0	0	0.3130 (0.3820)	−0.1758 (−0.1830)	−0.2165 (−0.2215)	0
$\dot{\varphi}$ (rad/s)	0	0	0	0	0	1	0	0

Table 20. CFD–RANS (extrapolated) 8 × 8 stability matrix for flight condition 14 in Tables 4 and 22 (reference takeoff case).

Variable	u/u_0	w/u_0	q (rad/s)	θ (rad)	v/u_0	p (rad/s)	r (rad/s)	φ (rad)
$\dot{u}/u_0$ (s^{-1})	−0.0396 (−0.0393)	0.1558 (0.1541)	−0.0041 (−0.0069)	−0.3113 (−0.3108)	0	0	0	0
$\dot{w}/u_0$ (s^{-1})	−0.1609 (−0.1596)	−0.5951 (−0.5939)	0.9835 (0.9719)	0	0	0	0	0
$\dot{q}$ (rad/s^2)	−0.1471 (−0.1474)	−0.2143 (−1.3645)	−0.6193 (−0.6861)	0	0	0	0	0
$\dot{\theta}$ (rad/s)	0	0	1	0	0	0	0	0
$\dot{v}/u_0$ (s^{-1})	0	0	0	0	−0.1163 (−0.1152)	0.0883 (0.1084)	−0.9889 (−0.9848)	0.1546 (0.1532)
$\dot{p}$ (rad/s^2)	0	0	0	0	−3.4185 (−3.4457)	−1.8573 (−1.8621)	1.0885 (1.2302)	0
$\dot{r}$ (rad/s^2)	0	0	0	0	0.2428 (0.3820)	−0.1690 (−0.1830)	−0.2127 (−0.2215)	0
$\dot{\varphi}$ (rad/s)	0	0	0	0	0	1	0	0

Table 21. CFD–RANS (extrapolated) 8 × 8 stability matrix for flight condition 15 in Tables 4 and 22 (reference takeoff case).

Variable	u/u_0	w/u_0	q (rad/s)	θ (rad)	v/u_0	p (rad/s)	r (rad/s)	φ (rad)
$\dot{u}/u_0$ (s^{-1})	−0.0354 (−0.0353)	0.1609 (0.1546)	−0.0064 (−0.0062)	−0.3207 (−0.3117)	0	0	0	0
$\dot{w}/u_0$ (s^{-1})	−0.1336 (−0.1294)	−0.5363 (−0.5957)	0.9773 (0.8765)	0	0	0	0	0
$\dot{q}$ (rad/s^2)	−0.1065 (−0.1325)	−1.3602 (−1.3687)	−0.6141 (−0.6187)	0	0	0	0	0
$\dot{\theta}$ (rad/s)	0	0	1	0	0	0	0	0
$\dot{v}/u_0$ (s^{-1})	0	0	0	0	−0.1031 (−0.1152)	0.1213 (0.0978)	−0.9850 (−0.8881)	0.1426 (0.1532)
$\dot{p}$ (rad/s^2)	0	0	0	0	−3.4887 (−3.4457)	−1.6699 (−1.8621)	1.1562 (1.2302)	0
$\dot{r}$ (rad/s^2)	0	0	0	0	0.4077 (0.3820)	−0.1566 (−0.1650)	−0.2096 (−0.1998)	0
$\dot{\varphi}$ (rad/s)	0	0	0	0	0	1	0	0

Table 22. CFD–RANS (extrapolated) 8 × 8 stability matrix for flight condition 16 in Tables 4 and 22 (reference takeoff case).

Variable	u/u_0	w/u_0	q (rad/s)	θ (rad)	v/u_0	p (rad/s)	r (rad/s)	φ (rad)
$\dot{u}/u_0$ (s^{-1})	−0.0356 (−0.0353)	0.1614 (0.1544)	−0.0051 (−0.0062)	−0.3207 (−0.3113)	0	0	0	0
$\dot{w}/u_0$ (s^{-1})	−0.1341 (−0.1292)	−0.5364 (−0.5950)	0.9820 (0.8753)	0	0	0	0	0
$\dot{q}$ (rad/s^2)	−0.1065 (−0.1325)	−0.7852 (−1.3670)	−0.5798 (−0.6179)	0	0	0	0	0
$\dot{\theta}$ (rad/s)	0	0	1	0	0	0	0	0
$\dot{v}/u_0$ (s^{-1})	0	0	0	0	−0.1036 (−0.1152)	0.1106 (0.0976)	−0.9871 (−0.8869)	0.1432 (0.1532)
$\dot{p}$ (rad/s^2)	0	0	0	0	−3.4705 (−3.4457)	−1.6679 (−1.6769)	1.0894 (1.1079)	0
$\dot{r}$ (rad/s^2)	0	0	0	0	0.3402 (0.3820)	−0.1494 (−0.1648)	−0.2046 (−0.1995)	0
$\dot{\varphi}$ (rad/s)	0	0	0	0	0	1	0	0

Table 23. CFD–RANS (extrapolated) 8 × 8 stability matrix for flight condition 17 in Tables 4 and 22 (reference takeoff case).

Variable	u/u_0	w/u_0	q (rad/s)	θ (rad)	v/u_0	p (rad/s)	r (rad/s)	φ (rad)
$\dot{u}/u_0$ (s^{-1})	−0.0306 (−0.0353)	0.1703 (0.1548)	−0.0053 (−0.0062)	−0.3299 (−0.3122)	0	0	0	0
$\dot{w}/u_0$ (s^{-1})	−0.1420 (−0.1295)	−0.5375 (−0.5966)	0.9821 (−0.8776)	0	0	0	0	0
$\dot{q}$ (rad/s^2)	−0.0307 (−0.1327)	−0.7719 (−1.3707)	−0.5722 (−0.6196)	0	0	0	0	0
$\dot{\theta}$ (rad/s)	0	0	1	0	0	0	0	0
$\dot{v}/u_0$ (s^{-1})	0	0	0	0	−0.1025 (−0.1152)	0.1321 (0.0979)	−0.9843 (−0.8893)	0.1511 (0.1532)
$\dot{p}$ (rad/s^2)	0	0	0	0	−3.5345 (−3.4457)	−1.6732 (−1.6815)	1.1669 (1.1109)	0
$\dot{r}$ (rad/s^2)	0	0	0	0	0.3155 (0.3820)	−0.1704 (−0.1653)	−0.2003 (−0.2000)	0
$\dot{\varphi}$ (rad/s)	0	0	0	0	0	1	0	0

Table 24. CFD–RANS (extrapolated) 8 × 8 stability matrix for flight condition 18 in Tables 4 and 22 (reference takeoff case).

Variable	u/u_0	w/u_0	q (rad/s)	θ (rad)	v/u_0	p (rad/s)	r (rad/s)	φ (rad)
$\dot{u}/u_0$ (s^{-1})	−0.0357 (−0.0353)	0.1620 (0.1542)	−0.0038 (−0.0062)	−0.3207 (−0.3110)	0	0	0	0
$\dot{w}/u_0$ (s^{-1})	−0.1347 (−0.1290)	−0.5364 (−0.5943)	0.9866 (0.8742)	0	0	0	0	0
$\dot{q}$ (rad/s^2)	−0.1065 (−0.1325)	−0.2096 (−1.3654)	−0.5552 (−0.6172)	0	0	0	0	0
$\dot{\theta}$ (rad/s)	0	0	1	0	0	0	0	0
$\dot{v}/u_0$ (s^{-1})	0	0	0	0	−0.1042 (−0.1152)	0.1001 (0.0975)	−0.9891 (−0.8859)	0.1437 (0.1532)
$\dot{p}$ (rad/s^2)	0	0	0	0	−3.4526 (−3.4457)	−1.6659 (−1.6750)	1.0236 (1.1066)	0
$\dot{r}$ (rad/s^2)	0	0	0	0	0.2714 (0.3820)	−0.1426 (−0.1646)	−0.2007 (−0.1992)	0
$\dot{\varphi}$ (rad/s)	0	0	0	0	0	1	0	0

Table 25. CFD–RANS (extrapolated) 8 × 8 stability matrix for flight condition 19 in Tables 4 and 22 (reference takeoff case).

Variable	u/u_0	w/u_0	q (rad/s)	θ (rad)	v/u_0	p (rad/s)	r (rad/s)	φ (rad)
$\dot{u}/u_0$ (s^{-1})	−0.0315 (−0.0327)	0.1646 (0.1547)	−0.0060 (−0.0058)	−0.3255 (−0.3120)	0	0	0	0
$\dot{w}/u_0$ (s^{-1})	−0.1163 (−0.1108)	−0.4963 (−0.5962)	0.9806 (0.8113)	0	0	0	0	0
$\dot{q}$ (rad/s^2)	−0.0825 (−0.1225)	−1.3566 (−1.3697)	−0.5661 (−0.5727)	0	0	0	0	0
$\dot{\theta}$ (rad/s)	0	0	1	0	0	0	0	0
$\dot{v}/u_0$ (s^{-1})	0	0	0	0	−0.0950 (−0.1152)	0.1282 (0.0905)	−0.9852 (−0.8221)	0.1341 (0.1532)
$\dot{p}$ (rad/s^2)	0	0	0	0	−3.5135 (−3.4457)	−1.5408 (−1.5544)	1.0940 (1.0269)	0
$\dot{r}$ (rad/s^2)	0	0	0	0	0.4252 (0.3820)	−0.1393 (−0.1528)	−0.2003 (−0.1849)	0
$\dot{\varphi}$ (rad/s)	0	0	0	0	0	1	0	0

Table 26. CFD–RANS (extrapolated) 8 × 8 stability matrix for flight condition 20 in Tables 4 and 22 (reference takeoff case).

Variable	u/u_0	w/u_0	q (rad/s)	θ (rad)	v/u_0	p (rad/s)	r (rad/s)	φ (rad)
$\dot{u}/u_0$ (s^{-1})	−0.0316 (−0.0326)	0.1652 (0.1545)	−0.0048 (−0.0057)	−0.3255 (−0.3116)	0	0	0	0
$\dot{w}/u_0$ (s^{-1})	−0.1167 (−0.1106)	−0.4964 (−0.5954)	0.9846 (0.8101	0	0	0	0	0
$\dot{q}$ (rad/s^2)	−0.0825 (−0.1225)	−0.7820 (−1.3679)	−0.5347 (−0.5719)	0	0	0	0	0
$\dot{\theta}$ (rad/s)	0	0	1	0	0	0	0	0
$\dot{v}/u_0$ (s^{-1})	0	0	0	0	−0.0956 (−0.1152)	0.1172 (0.0904)	−0.9873 (−0.8209)	0.1346 (0.1532)
$\dot{p}$ (rad/s^2)	0	0	0	0	−3.4925 (−3.4457)	−1.5390 (−1.5521)	1.0308 (1.0254)	0
$\dot{r}$ (rad/s^2)	0	0	0	0	0.3584 (0.3820)	−0.1322 (−0.1525)	−0.1954 (−0.1846)	0
$\dot{\varphi}$ (rad/s)	0	0	0	0	0	1	0	0

Table 27. CFD–RANS (extrapolated) 8 × 8 stability matrix for flight condition 21 in Tables 4 and 22 (reference takeoff case).

Variable	u/u_0	w/u_0	q (rad/s)	θ (rad)	v/u_0	p (rad/s)	r (rad/s)	φ (rad)
$\dot{u}/u_0$ (s^{-1})	−0.0317 (−0.0326)	0.1656 (0.1543)	−0.0035 (0.0057)	−0.3255 (−0.3112)	0	0	0	0
$\dot{w}/u_0$ (s^{-1})	−0.1171 (−0.1105)	−0.4965 (−0.5946)	0.9886 (0.8091)	0	0	0	0	0
$\dot{q}$ (rad/s^2)	−0.0825 (−0.1225)	−0.2068 (−1.3662)	−0.5122 (−0.5712)	0	0	0	0	0
$\dot{\theta}$ (rad/s)	0	0	1	0	0	0	0	0
$\dot{v}/u_0$ (s^{-1})	0	0	0	0	−0.0961 (−0.1152)	0.1064 (0.0902)	−0.9892 (−0.8198)	0.1350 (0.1532)
$\dot{p}$ (rad/s^2)	0	0	0	0	−3.4719 (−3.4457)	−1.5372 (−1.5502)	0.9686 (1.0241)	0
$\dot{r}$ (rad/s^2)	0	0	0	0	0.2903 (0.3820)	−0.1256 (−0.1523)	−0.1914 (−0.1844)	0
$\dot{\varphi}$ (rad/s)	0	0	0	0	0	1	0	0

Table 28. CFD–RANS (extrapolated) 8 × 8 stability matrix for flight condition 22 in Tables 4 and 22 (reference takeoff case).

Variable	u/u_0	w/u_0	q (rad/s)	θ (rad)	v/u_0	p (rad/s)	r (rad/s)	φ (rad)
$\dot{u}/u_0$ (s^{-1})	−0.0389 (−0.0271)	0.1703 (0.1542)	−0.0051 (−0.0049)	−0.3203 (−0.3108)	0	0	0	0
$\dot{w}/u_0$ (s^{-1})	−0.1453 (−0.0793)	−0.5559 (−0.5940)	0.9815 (0.6851)	0	0	0	0	0
$\dot{q}$ (rad/s^2)	−0.0404 (−0.1018)	0.7723 (−1.3648)	−0.5723 (−0.4836)	0	0	0	0	0
$\dot{\theta}$ (rad/s)	0	0	1	0	0	0	0	0
$\dot{v}/u_0$ (s^{-1})	0	0	0	0	−0.0993 (−0.1107)	0.1283 (0.0764)	−0.9851 (−0.6942)	0.1451 (0.1472)
$\dot{p}$ (rad/s^2)	0	0	0	0	−3.5230 (−3.3116)	−1.6723 (−1.3126)	1.1529 (0.8672)	0
$\dot{r}$ (rad/s^2)	0	0	0	0	0.3190 (0.3671)	−0.1667 (−0.1290)	−0.2009 (−0.1561)	0
$\dot{\varphi}$ (rad/s)	0	0	0	0	0	1	0	0

4.2. Relative Accuracy of Extrapolation versus CFD–RANS

Tables 29–32 for longitudinal and lateral stability derivatives at landing (takeoff) compare the extrapolated values $\overline{C}_{Xi}$ versus direct CFD–RANS values C_{Xi}, preferring relative (52b) to absolute (52a) differences as related by (52b):

$$\Delta C_{Xi} \equiv C_{Xi} - \overline{C}_{Xi}, \tag{52a}$$

$$\delta C_{Xi} = \frac{|\Delta C_{Xi}|}{|\overline{C}_{Xi}|} = \left|\frac{C_{Xi}}{\overline{C}_{Xi}}\right| - 1 \tag{52b}$$

Table 29. Relative accuracy of landing longitudinal stability derivatives (percentage discrepancy % between extrapolation and CFD–RANS).

Flight Condition	C_{Xu}	C_{Zu}	C_{Mu}	C_{Xw}	C_{Zw}	C_{Mw}	C_{Xq}	C_{Zq}	C_{Mq}	$C_{X\theta}$	$C_{Z\theta}$	$C_{M\theta}$
2	−0.50	+0.05	0.00	+0.25	+0.17	−41.20	−20.25	+0.60	−5.29	+0.18	0.00	—
3	0.00	−0.16	−0.45	+0.49	+0.33	−82.61	−41.77	+1.18	−9.00	+0.31	+0.17	—
4	+0.55	0.00	+1.02	+9.82	0.00	+11.06	+5.63	+11.14	+0.07	+11.45	−100.00	—
5	+0.55	+0.26	+1.02	+1.17	−9.80	−41.20	−21.13	+12.38	−5.14	+0.55	−100.00	—
6	+4.44	−0.26	+92.35	+0.55	+11.28	−27.21	−21.13	+12.42	−4.81	+11.81	−100.00	—
7	+0.55	−0.14	+1.02	+1.17	−9.65	−82.61	−40.85	+12.72	−8.99	+0.67	−100.00	—
8	+0.55	−2.87	+1.57	+3.80	−11.12	0.00	+2.86	+13.18	0.00	+3.39	−100.00	—
9	+0.87	+0.21	+1.60	+1.29	+14.70	−21.05	−20.59	+17.43	−5.14	+35.21	−100.00	—
10	+0.29	−0.07	+4762.96	+2.10	−12.92	−82.51	−41.18	+18.13	−8.71	+9.07	−100.00	—
11	+27.50	−4.67	+143.37	−1.54	−6.48	+40.92	−27.03	+8.42	−0.81	+2.45	−100.00	—

Table 30. Relative accuracy of landing lateral stability derivatives (percentage discrepancy % between extrapolation and CFD–RANS).

Flight Condition	C_{Yv}	C_{Lv}	C_{Nv}	C_{Yp}	C_{Lp}	C_{Np}	C_{Yr}	C_{Lr}	C_{Nr}	$C_{Y\psi}$	$C_{L\psi}$	$C_{N\psi}$
2	+0.36	−0.26	−19.70	−10.47	−0.19	−5.52	+0.27	−5.95	−1.59	+0.06	—	—
3	+0.72	+0.50	−39.71	−20.70	−0.37	−10.62	+0.53	−11.79	−2.79	+0.17	—	—
4	−9.92	+0.20	+11.46	+11.97	−0.62	−11.68	+11.24	+0.46	+7.49	−9.97	—	—
5	−9.65	+0.14	−8.21	+0.52	−0.62	−16.09	+11.72	−5.39	+5.57	+0.25	—	—
6	−9.55	−0.30	−7.43	−1.83	−0.57	−17.61	+11.79	−6.15	+5.94	−0.19	—	—
7	−9.28	−0.46	−11.44	−11.01	−0.95	−21.29	−11.09	−11.09	+3.85	−9.80	—	—
8	−11.10	+0.29	+15.45	+13.53	−0.81	−14.51	+12.71	+0.56	+10.08	−11.11	—	—
9	−13.38	−0.08	−0.42	+5.35	−0.80	−19.79	+16.63	−5.23	+7.99	−13.62	—	—
10	−13.10	−0.42	−24.23	−6.45	−0.81	−24.81	+17.07	−10.93	+6.49	−13.56	—	—
11	−6.16	−6.48	+0.06	−8.39	−4.12	−22.34	+17.97	+7.39	+2.59	−7.59	—	—

Table 31. Relative accuracy of takeoff longitudinal stability derivatives (percentage discrepancy % between extrapolation and CFD–RANS).

Flight Condition	C_{Xu}	C_{Zu}	C_{Mu}	C_{Xw}	C_{Zw}	C_{Mw}	C_{Xq}	C_{Zq}	C_{Mq}	$C_{X\theta}$	$C_{Z\theta}$	$C_{M\theta}$
13	+0.51	+0.38	−0.14	+0.58	+0.12	−42.09	−20.29	+0.80	−5.67	+0.10	-	-
14	+0.76	+0.81	−0.20	+1.10	+0.20	−84.29	−40.57	+1.19	−9.74	+0.16	-	-
15	+0.28	+3.25	−19.62	+4.08	−9.97	−0.62	+3.23	+11.50	−0.74	+2.89	-	-
16	+0.85	+3.79	−19.62	+4.53	−9.85	−42.56	−17.74	+12.19	−6.17	+3.02	-	-
17	−13.31	+9.65	−76.87	+10.01	−9.91	−43.69	−14.52	+11.91	−7.65	+5.67	-	-
18	+1.13	+4.42	−19.62	+5.06	−9.74	−84.65	−38.71	+12.86	−10.05	+3.12	-	-
19	−3.67	+4.96	−32.65	+6.40	−16.76	−0.96	+3.45	+20.87	−1.15	+4.33	-	-
20	−3.07	+5.52	−32.05	+6.93	−16.63	−42.83	−15.79	+21.54	+6.51	+4.46	-	-
21	−2.76	+5.97	−32.65	+7.32	−16.50	−84.86	−38.66	+22.19	−10.33	+4.60	-	-
22	+43.54	+83.23	−60.31	+10.44	−6.41	−43.41	+4.08	+43.26	+18.34	+3.06	-	-

Table 32. Relative accuracy of takeoff lateral stability derivatives (percentage discrepancy % between extrapolation and CFD–RANS).

Flight Condition	C_{Yv}	C_{Lv}	C_{Nv}	C_{Yp}	C_{Lp}	C_{Np}	C_{Yr}	C_{Lr}	C_{Nr}	$C_{Y\psi}$	$C_{L\psi}$	$C_{N\psi}$
13	+0.52	−0.40	−18.06	−9.32	−0.13	−3.93	+0.21	+5.80	−2.26	+0.46	-	-
14	+0.95	−0.79	+34.44	−18.54	−0.26	−7.65	+0.41	−11.52	−3.97	+0.91	-	-
15	−10.50	+1.25	+6.73	+24.03	−10.32	−5.09	+10.91	−6.02	+4.90	−6.92	-	-
16	−10.06	+0.72	−10.94	+13.33	−0.54	−9.34	+11.30	−1.67	+2.56	−6.53	-	-
17	−11.02	+2.58	−17.41	+34.93	−0.49	+3.09	+10.68	+5.04	+0.15	−1.37	-	-
18	−9.55	+0.20	−28.95	+2.67	−0.54	−13.37	+11.65	−7.50	+0.75	−6.20	-	-
19	−17.53	+1.97	+11.31	+41.66	−0.87	−8.84	+19.84	+6.53	+8.33	−12.47	-	-
20	−17.01	+1.36	−6.18	+39.65	−0.84	−13.31	+20.27	+0.53	+5.88	−12.14	-	-
21	−16.58	+0.76	−24.01	+17.96	−0.84	−17.53	+20.66	−5.42	+3.80	−11.88	-	-
22	−10.30	+6.38	−13.10	+67.93	+27.40	+29.22	+41.90	+32.95	+28.70	−1.43	-	-

The relative differences (52b) were used as the basis for the validation of the extrapolation method versus the CFD–RANS results.

Table 29 for longitudinal derivatives at landing shows that of the derivatives of forces and moments with regard to longitudinal velocity, C_{Zu} was the most accurate, with discrepancies of less than 0.3% for flight conditions 2 to 10 without sideslip, except a discrepancy of less than 3% for flight condition 8. The discrepancy was larger but less than 5% for flight condition 12 with sideslip, with overall good results for the extrapolation factor (38). The stability derivative C_{Xu} also showed small discrepancies of less than 1% for all flight conditions 2 to 10 without sideslip, except flight condition 6 with a discrepancy of less than 5%. The sideslip in flight condition 11 led to a much larger discrepancy for the extrapolation factor (43a,b) that applied to the two stability derivatives $\{C_{Xu}, C_{Mu}\}$. The results for C_{Mu} showed small discrepancies of less than 2% for most flight conditions, but also very large deviations for flight conditions 6, 10, and 11. The stability matrices in Tables 11, 15 and 16 show that the CFD–RANS results differed substantially from the baseline flight condition 1 in Table 6, and thus an extrapolation method could not be expected to agree. The large differences in CFD–RANS data could have been due to a genuine physical phenomenon such as flow separation or reattachment, which could have a significant effect on pitching moment C_M and its derivative with regard to longitudinal velocity C_{Mu}, or they could have been outliers due to some numerical instability requiring further scrutiny of the computation.

The other stability derivatives in Table 29 showed better accuracies for C_{Xw} and larger deviation for C_{Zw} and C_{Mw} using the same simple extrapolation factor (40) for derivatives with regard to vertical velocity. The discrepancies of derivatives with regard to pitch rate vary widely with flight condition from four accurate digits to none at all. It should be noted that C_{Xq} was usually small ≤ 0.01, so small absolute errors such as 0.002 became large relative errors such as 20%; that was not the case for C_{Zq} and C_{Mq}, with values closer to unity and thus more representative relative errors. The derivative with regard to pitch angle $C_{X\theta}$ also varied in accuracy. The deviations of −100.00% for $C_{Z\theta}$ corresponded to cases in (52b) for which CFD–RANS gave zero $C_{Xi} = 0$ and the extrapolation gave a small nonzero value, so $\delta C_{Xi} = -1$ in (52b).

The lateral stability derivatives at landing in Table 30 showed the smallest discrepancies for C_{Lv}, of less than 0.5% for all flight conditions 2 to 10 without sideslip and larger but of less than 7% for flight condition 11 with sideslip, validating the extrapolation factor (46). The stability derivative C_{Lp} was also accurate, with discrepancies of less than 1% in flight conditions 2 to 10 without sideslip and less than 5% in flight condition 11 with sideslip using the extrapolation factor (30). Other lateral stability derivatives, some using similar extrapolation factors, showed discrepancies mostly in the range of 5 to 15% and rarely beyond 25%, which may be indicative of the expected accuracy of the extrapolation method in most cases.

Before proceeding to a more general statistical assessment of the accuracy of extrapolation versus CFD–RANS, the longitudinal (lateral) stability derivatives are considered not only for landing in Tables 29 and 30 but also for takeoff in Tables 31 and 32. The stability derivatives C_{Xu} and C_{Zu} were generally less accurate for takeoff (Table 31) than for landing (Table 29) while remaining mostly below 5% for flight conditions without sideslip. Flight conditions 11 and 22 with sideslip led to larger discrepancies between extrapolation and CFD–RANS for C_{Xu}, C_{Zu}, and C_{Mu}; the extreme cases for C_{Mu} at landing in Table 29 did not appear for takeoff in Table 31. Concerning the remaining longitudinal stability derivatives C_{Xw}, C_{Zw}, C_{Mw}, C_{Xq}, C_{Zq}, and C_{Mq}, their accuracies varied mostly in the same range of 5 to 20% for landing in Table 29 and takeoff in Table 31. There are few nonzero CFD–RANS values for $C_{Z\theta}$, and for $C_{X\theta}$. The accuracy was more consistently better at takeoff in Table 31 than at landing in Table 29.

Concerning the lateral stability derivatives at landing (takeoff) in Tables 30 and 32, the most accurate were: (i) C_{Lv} with extrapolation factor (46), with errors often less than 1% and never above 3% except for 5–6% in the flight conditions with sideslip; (ii) C_{Lp} with extrapolation factor (30), with errors of less than 1% in all flight conditions without sideslip except at takeoff, but with larger errors with sideslip, 4% at landing and 27% at takeoff. The remaining lateral stability derivatives C_{Yr}, C_{Nv}, C_{Yp}, C_{Np}, C_{Yr}, C_{Lr}, C_{Nr}, and $C_{Y\psi}$ showed comparable scatters of errors mostly in the 5–10% range for both landing (Table 30) and takeoff (Table 32). The comparison of accuracies for 420 stability derivatives in 20 matrices supported some statistical analysis (Section 4.3).

4.3. Validation of Stability for 20 Matrices and 420 Derivatives

Collectively, Tables 5–28 for landing (takeoff) compare 20 extrapolated matrices and 420 derivatives with CFD–RANS results and served as the basis for an overall assessment in Tables 29–38. Starting with the landing (takeoff) flight conditions 1 to 11 (12 to 22) in Table 4, the respective extrapolation factors in Tables 5 and 6, applied to the baseline flight condition 1 in Tables 7 and 8 and extrapolated to flight conditions 2 to 11 and Tables 12–22 in Tables 9–28, the comparison with CFD–RANS results in Tables 29 and 30 (Tables 31 and 32) leads to several assessments in Tables 33–38. Tables 33 and 34 has nine lines, showing the instances with accuracies in the ranges

$$0.00,\ 0.00\text{-}1.00,\ 1.00\text{-}2.00,\ 2.00\text{-}5.00,\ 5.00\text{-}10.0,\ 10.0\text{-}20.0,\ 20.0\text{-}30.0,\ 30.0\text{-}50.0,\ >50.0 \quad (53)$$

Table 33. Comparative accuracy of extrapolation and CFD–RANS (landing).

Discrepancy %	Number of Cases	Percentage of Cases	Cumulative Cases	Cumulative Percentage
0.00	7 + 0 = 7	6.86/0.00/3.47	7 + 0 = 7	6.86/0.00/3.47
0.00–1.00	28 + 31 = 59	27.45/31.00/29.21	35 + 31 = 66	34.31/31.00/32.67
1.00–2.00	10 + 2 = 12	9.80/2.00/5.94	45 + 33 = 78	44.12/33.00/38.61
2.00–5.00	8 + 5 = 13	7.84/5.00/6.44	53 + 38 = 91	51.96/38.00/45.05
5.00–10.00	12 + 25 = 37	11.76/25.00/18.32	65 + 63 = 128	63.73/63.00/63.37
10.00–20.00	16 + 31 = 47	15.69/31.00/23.27	81 + 94 = 175	79.41/94.00/86.63
20.00–30.00	8 + 5 = 13	7.84/5.00/6.44	89 + 99 = 188	87.25/99.00/93.07
30.00–50.00	7 + 1 = 8	6.86/1.00/3.96	96 + 100 = 196	94.12/100.00/97.03
>50.00	6 + 0 = 6	5.88/0.00/2.91	102 + 100 = 202	100.00/100.00/100.00
Total	102 + 100 = 202	100.00/100.00/100.00	—	—

Longitudinal + lateral = total.

There are four columns indicating: (i),(ii) the number of cases in each range (53) and the percentage of total; (iii),(iv) the cumulative number of cases with accuracy with upper limits (53) and the percentage of the total. In each column are separated the longitudinal and lateral derivatives in the sum. For example, for stability derivatives at landing in Table 33 the extrapolation was exact, with four accurate digits (discrepancy 0.00%), in seven cases for longitudinal derivatives and none for lateral derivatives. The errors were

nonzero but less than 1% for 28 longitudinal (31 lateral) stability derivatives, corresponding to 27.45% (31.00%) of the total of 102 longitudinal (100 lateral) stability derivatives. Thus, of the total of 202 longitudinal plus lateral stability derivatives, 7 (3.47%) had zero error and 59 (29.21%) had nonzero error less than 1%. In cumulative terms, the error did not exceed 5% for 53 longitudinal (38 lateral) stability derivatives (corresponding to 51.96% (30.00%) of the total of 102 (100)); considering the aggregate of longitudinal and lateral stability derivatives, of a total of 202 cases, the error was less than 5% in 91 cases (45.05%), less than 10% in 128 cases (63.37%), and less than 20% in 175 cases (86.63%). Similar statistics as in Table 33 for landing flight conditions appear in Table 34 for takeoff flight conditions, for example, error of less than 5% for 78 cases (39.00%) out of a total of 200, less than 10% for 115 cases (57.50%), and less than 20% for 161 cases (80.50%). Most stability derivatives were estimated with accuracies of 10% or better using the simple extrapolation factors provided.

Table 34. Comparative accuracy of extrapolation and CFD–RANS (takeoff).

Discrepancy %	Number of Cases	Percentage of Cases	Cumulative Cases	Cumulative Percentage
0.00	0 + 0 = 0	0.00/0.00/0.00	0 + 0 = 7	0.00/0.00/0.00
0.00–1.00	17 + 22 = 39	17.00/22.00/19.50	17 + 22 = 39	17.00/22.00/19.50
1.00–2.00	4 + 6 = 10	4.00/6.00/5.00	21 + 28 = 49	21.00/28.00/29.50
2.00–5.00	20 + 9 = 29	10.00/9.00/14.50	41 + 37 = 78	41.00/37.00/39.00
5.00–10.00	17 + 20 = 37	17.00/20.00/18.50	58 + 57 = 115	58.00/57.00/57.50
10.00–20.00	20 + 26 = 46	20.00/26.00/23.00	78 + 83 = 161	78.00/83.00/80.50
20.00–30.00	4 + 8 = 12	4.00/8.00/6.00	82 + 91 = 173	82.00/91.00/97.00
30.00–50.00	13 + 8 = 21	13.00/8.00/10.50	95 + 99 = 194	95.00/99.00/97.00
>50.00	5 + 1 = 6	5.00/1.00/3.00	100 + 100 = 200	100.00/100.00/100.00
Total	100 + 100 = 200	100.00/100.00/100.00	—	—

Longitudinal + lateral = total derivative.

Table 35. Comparison of extrapolation with CFD–RANS (landing).

Stability Derivative	Range of Values		Relative Deviation (%)
	CFD–RANS	Extrapolation	
C_{Xu}	−0.0401/−0.0459	−0.03451/−0.0403	−0.50/+4.44
C_{Zu}	−0.1415/−0.1902	−0.1412/−0.1902	−2.87/+0.26
C_{Mu}	−0.218/−0.9191	−0.0186/−0.0218	−0.45/+1.60
C_{Xw}	+0.1602/+0.1694	+0.1487/+0.1629	−1.54/+10.15
C_{Zw}	−0.5002/−0.5865	−0.4745/−0.5865	−12.92/+14.70
C_{Mw}	−0.2248/−1.2966	−1.04921/−1.2966	−82.61/+40.92
C_{Xq}	−0.0040/−0.0079	−0.0068/−0.0079	−41.77/+5.63
C_{Zq}	+0.9723/+0.9880	+0.8364/+0.9723	+0.60/+17.43
C_{Mq}	−0.5033/−0.6409	−0.5513/−0.6409	−9.00/+0.07
$C_{X\theta}$	−0.03190/−0.3309	−0.2946/−0.3278	+0.19/+35.21
C_{Yv}	−0.0952/−0.1099	−0.1023/−0.1099	−13.38/+0.72
C_{Lv}	−3.1950/−3.2172	−2.9880/−3.2109	−6.48/+0.50
C_{Nv}	+0.2427/+0.3570	+0.2881/+0.3203	+15.45/−39.71
C_{Yp}	+0.1030/+0.1292	+0.1101/+1.280	−20.70/+13.53
C_{Lp}	−1.5342/−1.7988	−1.5467/−1.7980	−0.19/−4.12
C_{Np}	−0.1279/−0.1977	−0.1701/−0.1840	−5.52/−22.34
C_{Yr}	−0.9822/−0.9891	−0.8462/−0.9822	+0.27/+17.07
C_{Lr}	+1.0460/+1.3652	+1.059/1.3652	−11.79/+7.39
C_{Nr}	−0.1786/−0.2076	−0.1786/−0.2076	−2.79/+10.08
$C_{Y\psi}$	+0.1509/+0.1755	+0.1577/+0.1755	−13.62/+0.17

Table 36. Comparison of extrapolation with CFD–RANS (takeoff).

Stability Derivative	Range of Values		Relative Deviation (%)
	CFD–RANS	Extrapolation	
C_{Xu}	−0.03061/−0.0396	−0.0271/−0.0393	−13.31/+43.54
C_{Zu}	−0.1163/−0.1609	−0.07931/−0.1596	+0.38/+83.23
C_{Mu}	−0.0307/−0.1471	−0.1018/−0.1473	−0.14/−60.31
C_{Xw}	+0.1544/+0.5703	+0.1541/+0.1548	+0.58/+10.44
C_{Zw}	−0.4963/−0.5951	−0.5939/−0.5966	−16.76/+0.12
C_{Mw}	−0.2068/−1.3668	−1.3566/−1.3707	−0.62/−84.65
C_{Xq}	−0.0035/−0.0069	−0.0049/−0.0069	−40.57/+17.74
C_{Zq}	+0.9719/+0.9886	+0.6851/+0.9719	+0.60/+43.26
C_{Mq}	−0.5122/−0.6861	−0.4836/−0.6861	−10.33/+18.34
$C_{X\theta}$	−0.3113/−0.3299	−0.3108/−0.3122	+0.10/+4.60
C_{Yv}	−0.0950/−0.1163	−0.1107/−0.1152	−17.53/+0.95
C_{Lv}	−3.4185/−3.5230	−3.3116/−3.4457	−0.79/+6.38
C_{Nv}	+0.2428/+0.4252	+0.3671/+0.3820	−34.44/+11.31
C_{Yp}	+0.0883/−0.1321	+0.0764/+0.1084	−18.54/+67.73
C_{Lp}	−1.5372/−1.8621	−1.3126/−1.8621	−0.13/+27.40
C_{Np}	−0.1256/−0.1830	−0.1290/−0.1830	−17.53/+29.22
C_{Yr}	−0.9848/−0.9892	−0.6942/−0.9848	+0.21/+41.90
C_{Lr}	+0.9686/+1.2302	+0.8672/+1.2302	−11.52/+32.95
C_{Nr}	−0.1914/−0.2215	−0.1561/−0.2215	−3.97/+28.70
$C_{Y\psi}$	+0.1341/+0.1532	+0.1472/+0.1532	−12.47/+0.91

Table 37. Comparison of consistency of stability derivatives (landing).

Relative Deviation	Stability Derivative	Number
<5%	C_{Xu}, C_{Zu}, C_{Mu}, C_{Xw}, C_{Lp}	5
5–10%	C_{Xq}, C_{Mq}, C_{Lv}, C_{Nr}	4
10–20%	C_{Zw}, C_{Zq}, C_{Yv}, C_{Yp}, C_{Yr}, C_{Lr}, $C_{Y\psi}$	7
20–50%	$C_{X\theta}$, C_{Nv}, C_{Np}	3
>50%	C_{Mw}	1
		Total = 20

Table 38. Comparison of consistency of stability derivatives (takeoff).

Relative Desviation	Stability Derivative	Number
<5%	—	0
5–10%	C_{Xw}, $C_{X\theta}$, C_{Lv}	3
10–20%	C_{Zw}, C_{Mq}, C_{Yv}, $C_{Y\psi}$	4
20–50%	C_{Xu}, C_{Xq}, C_{Zq}, C_{Nv}, C_{Lp}, C_{Np}, C_{Yr}, C_{Lr}, C_{Nr}	9
>50%	C_{Zu}, C_{Mu}, C_{Mw}, C_{Yp},	4
		Total = 20

The average values of discrepancies were not very significant, because the accuracy of extrapolation varied widely among stability derivatives, as can be seen in Tables 35 and 36 for the landing (takeoff) case, which show for all stability derivatives: (i) the extrapolated value; (ii) the CFD–RANS result; (iii) the percentage deviation. Tables 35 and 36 allowed the identification of the most and least accurate stability derivatives in Tables 37 and 38. For the landing case in Table 37, five stability derivatives, C_{Xu}, C_{Zu}, C_{Mu}, C_{Xw}, and C_{Lp}, are quite accurate (<5% error) in all flight conditions, bearing in mind the simplicity of the extrapolation. Another four stability derivatives, C_{Xq}, C_{Mq}, C_{Lv}, and C_{Nr}, with errors of less than 10% in all cases, are still usable. The seven stability derivatives C_{Zw}, C_{Zq}, C_{Yv}, C_{Yp}, C_{Lr}, and $C_{Y\psi}$ with errors of 10 to 20%, require caution and comparison with other methods. The most inaccurate extrapolations are $C_{X\theta}$, C_{Nv}, and C_{Np}, with errors of 20 to 50%, and C_{Mw}, with error of more than 50% in some flight conditions. Comparison with Table 38 for

the takeoff shows that no stability derivative achieved better than 5% accuracy in all flight cases, although this was due to a few cases, as can be seen in Tables 34 and 36. Accuracies of 5 to 10% are obtained for three stability derivatives, C_{Xw}, $C_{X\theta}$, and C_{Lv}; errors of 10 to 20% for a further four stability derivatives, C_{Zw}, C_{Mq}, C_{Yv}, $C_{Y\psi}$; errors of 20 to 50% for the majority of nine stability derivatives, C_{Xu}, C_{Xq}, C_{Zq}, C_{Nv}, C_{Lp}, C_{Np}, C_{Yr}, C_{Lr} and C_{Nr}; and error of more than 50% for four stability derivatives, C_{Zu}, C_{Mu}, $C_{M\dot{w}}$, and C_{Yp}. Comparison of Tables 37 and 38 for landing (takeoff) suggests that the extrapolation method works better for the former, but in fact this is due to a small number of cases. Comparison of all landing (takeoff) cases in Tables 29, 31 and 32 show comparable accuracies, though not always for the same derivatives. The accuracies better than 10% apply to C_{Xw} and C_{Lv} at landing and takeoff, to $C_{X\theta}$ only at takeoff, and to C_{Xu}, C_{Zu}, C_{Mu}, C_{Lp}, C_{Xq}, C_{Mq}, and C_{Nr} only at landing. The comparison of 420 extrapolations with CFD–RANS results in 20 complete longitudinal plus lateral stability matrices, which supports some conclusions (Section 5).

5. Conclusions

The linearization of the mathematical model of a rigid symmetric aircraft (Section 2) readily supplies the decoupled longitudinal and lateral stability matrices, involving 24 non-trivial stability derivatives different from zero or unity in the dimensionless longitudinal (21) and lateral (22) stability matrices. In order to obtain stability derivatives with an accuracy of, say, 10%, the forces and moments must be determined with an accuracy of about 3%. This sets a requirement for high fidelity in computational fluid mechanics calculations that may be difficult to achieve in partially separated flow conditions that can occur at takeoff and landing. The same level of accuracy in measurements in a wind tunnel requires a high-quality model in a suitably large cross-section with well-controlled flow. Both the computational and experimental approaches can be expensive. Repeating runs for a table of combinations of airspeed, AoA, and AoS for each of 24 stability derivatives represents a significant effort. This effort can be substantially reduced by the availability of formulas for the dependence of the stability derivatives on the airspeed, AoA, and AoS.

The present paper represents a first step in this direction, and the extrapolation factors obtained can undoubtedly be improved upon by a more refined analysis. The simple formulas for the dependence of stability derivatives on the airspeed, AoA, and AoS in Tables 1 and 2 can have a wide range of applications; they allow the extrapolation of stability derivatives for moderate changes in airspeed, AoA, and AoS. The results obtained for the 22 flight cases in Table 4 of a V-tailed aircraft (Table 3 and Figure 1) show that for moderate changes in AoA of up to 10° in (54a), changes in AoS of up to 15° in (54b), and changes in airspeed of up to 15% in (54c):

$$\Delta\alpha \equiv |\alpha_1 - \alpha_2| < 10^\circ \tag{54a}$$

$$\Delta\beta \equiv |\beta_1 - \beta_2| < 15^\circ \tag{54b}$$

$$\delta V \equiv |U - 1| = |V_2/V_1 - 1| < 0.15 \tag{54c}$$

the extrapolation factors for stability derivatives in Table 1 provide for landing (takeoff) the orders of accuracy indicated in Tables 7–38. The results obtained show the potential uses of formulas specifying the dependence of the stability derivatives on the airspeed, AoA, and AoS to reduce the wind tunnel measurement or high-fidelity CFD effort by allowing: (i) the extrapolation of a list of dependence on AoA for a fixed AoS to other values of the AoS, filling a complete table; (ii) the table could alternatively be filled from a list of dependence on AoS at fixed AoA extrapolated to other AoA; (iii) the ultimate combined extrapolation would start with a single value of the stability derivative at fixed AoA and AoS and then be extended to a table of (nonzero) combinations of both. The dependence on airspeed adds a third dimension to the AoA and AoS table.

The dependence of the stability derivatives on airspeed, AoA, and AoS uses only the dependence of the aerodynamic forces and moments on the square of velocity, which is

valid only for subsonic potential flow, insensitive to compressibility and viscosity; taking the latter into account introduces further dependence on the velocity through the Mach and Reynolds numbers for high and low velocities, respectively. Stability derivatives were compared for the same aircraft configuration at different airspeeds, AoAs, and AoS. Comparisons were made for different flight conditions with the same configuration (landing or takeoff) of the same aircraft. Some extrapolations of stability derivatives were reasonably accurate and others far off the mark in a fairly large validation set based on CFD–RANS that may not have been totally infallible. In any case, checking extrapolated stability derivatives against other methods is advisable. The present first approach to extrapolation of stability derivatives showed both promise, in some encouraging and accurate results, and plenty of scope for improvement, in other cases. Not too much should be expected of simple analytical extrapolation formulas. The reasoning used to derive the extrapolation formulas was approximate and far from unique, leaving plenty of scope for alternative approaches.

Author Contributions: Conceptualization, L.M.B.C.C.; methodology, L.M.B.C.C.; formal analysis, L.M.B.C.C. and J.M.G.M.; resources, L.M.B.C.C. and J.M.G.M.; writing—original draft preparation, L.M.B.C.C. and J.M.G.M.; writing—review and editing, L.M.B.C.C. and J.M.G.M.; visualization, L.M.B.C.C. and J.M.G.M.; project administration, L.M.B.C.C. and J.M.G.M. All authors have read and agreed to the published version of the manuscript.

Funding: This work was started during the project NEFA (New Empennage for Aircraft) of the European Union aeronautics program (2003–2005) under the European Research Contract No. G4RD-CT-2002-00864. It was continued and was supported by Fundação para a Ciência e a Tecnologia (FCT) through IDMEC, under LAETA, project UIDB/50022/2020.

Institutional Review Board Statement: Not applicable.

Informed Consent Statement: Not applicable.

Data Availability Statement: Data sharing not applicable.

Acknowledgments: This work was started under the NEFA project and benefited from comments of other partners in this activity.

Conflicts of Interest: The authors declare no conflict of interest.

Glossary

c	mean aerodynamic chord (20)
C_{Xi}	stability derivative calculated by CFD–RANS
$\overline{C}_{Xi}$	stability derivative calculated by extrapolation method
f_i	correction factors for stability derivatives (i = 0, u, w, α, β)
$\vec{g}$	acceleration of gravity (1)
$\vec{G}$	moment of forces (2)
I_{ij}	inertia matrix (7)
L	x-component of moment (4b)
M	y-component of moment (4b)
N	z-component of moment (4b)
p	x-component of angular velocity (5)
$\vec{P}$	linear momentum (6)
$\dot{\vec{P}}$	time rate of linear momentum or inertia force (1)
q	y-component of angular velocity (5)
$\vec{Q}$	angular momentum (8)
$\dot{\vec{Q}}$	time rate of angular momentum (2)
r	z-component of angular velocity (5)
R_{ij}	radii of gyration (7)
S	wing area (18)

u	x-component of linear velocity (6)
v	y-component of linear velocity (6)
V	linear velocity (6)
w	z-component of linear velocity (6)
u_0, v_0, w_0	components of mean velocity (12)
X	x-component of force (4a)
Y	y-component of force (4a)
Z	z-component of force (4a)
α	angle of attack (AoA)
β	angle of sideslip (AoS)
δ	deflection of control surface (20)
θ	pitch attitude (3)
φ	bank angle (3)
ψ	track angle (5)
ρ	mass density of air (16)
$\vec{\Omega}$	angular velocity (2)

Superscripts

$\dot{X}$	time derivative of X

Subscripts for control surface deflection

a	aileron
l	left tail
r	right tail

Abbreviations

AoA	angle of attack
AoS	angle of sideslip
CFD	computational fluid dynamics
l.h.s.	left-hand side
m.a.c.	mean aerodynamic chord
RANS	Reynolds-averaged Navier–Stokes
r.h.s.	right-hand side

References

1. Von Mises, R. *Theory of Flight*; McGraw-Hill: New York, NY, USA, 1945.
2. Perkins, C.D.; Hage, R.E. *Airplane, Performance, Stability and Control*; Wiley: Hoboken, NJ, USA, 1949.
3. Rabister, W. *Aircraft Dynamic Stability and Response*; Pergamon: London, UK, 1960.
4. Miele, A. *Flight Mechanics: Theory of Flight Paths*; Addison-Wesley: New York, NY, USA, 1962.
5. Etkin, B. *Dynamics of Atmospheric Fight*; Wiley: Hoboken, NJ, USA, 1972.
6. McRuer, D.; Ashkenas, I.; Graham, D. *Aircraft Dynamics and Automatic Control*; Princeton University Press: Princeton, NJ, USA, 1973.
7. Etkin, B.; Reid, L.D. *Dynamics of Flight: Stability and Control*, 3rd ed.; Wiley: Nova York, NY, USA, 1995.
8. Nelson, R.C. *Flight Stability and Automatic Control*, 2nd ed.; McGraw-Hill: New York, NY, USA, 1998.
9. Tischler, M.B. *Advances in Flight Control*; Taylor & Francis: London, UK, 1996.
10. Abzug, M.J.; Larrabee, E.E. *Airplane Stability and Control*, 2nd ed.; Cambridge University Press: Nova York, NY, USA, 2002.
11. Vatandaş, E.; Anteplıoğlu, A. Aerodynamic performance comparison of V-tail and conventional tail for an unmanned vehicle. In Proceedings of the 7th International Conference on Recent Advances in Space Technologies (RAST), Istanbul, Turkey, 16–19 June 2015; pp. 655–658.
12. Ciliberti, D.; Pierluigi, D.V.; Nicolosi, F.; Agostino, D.M. Aircraft directional stability and vertical tail design: A review of semi-empirical methods. *Prog. Aerosp. Sci.* **2017**, *95*, 140–172. [CrossRef]
13. Sánchez-Carmona, A.; Cuerno-Rejado, C.; García-Hernández, L. Unconventional tail configurations for transport aircraft. *Prog. Flight Phys.* **2017**, *9*, 127–148.
14. Sánchez-Carmona, A.; Cuerno-Rejado, C. Vee-tail conceptual design criteria for commercial transport aeroplanes. *Chin. J. Aeronaut.* **2019**, *32*, 595–610. [CrossRef]
15. García-Hernández, L.; Cuerno-Rejado, C.; Pérez-Cortés, M. Dynamics and Failure Models for a V-Tail Remotely Piloted Aircraft System. *J. Guid. Control. Dyn.* **2018**, *41*, 505–513. [CrossRef]
16. Campos, L.M.B.C. *Aircraft Design Integration and Affordability*; Report 826; Advisory Group for Aerospace Research & Development: Paris, France, 1998.
17. Torenbeek, E. *Advanced Aircraft Design—Conceptual Design, Analysis and Optimization of Subsonic Civil Airplanes*; John Wiley and Sons, Ltd.: Chichester, UK, 2013.

18. Obert, E. *Aerodynamic Design of Transport Aircraft*; IOS Press: Delft, The Netherlands, 2009.
19. Campos, L.M.B.C. On Physical Aeroacoustics with Some Implications for Low-Noise Aircraft Design and Airport Operations. *Aerospace* **2015**, *2*, 17–90. [CrossRef]
20. Okonkwo, P.; Smith, H. Review of evolving trends in blended wing body aircraft design. *Prog. Aerosp. Sci.* **2016**, *82*, 1–23. [CrossRef]
21. Kozek, M.; Schirrer, A. *Modeling and Control for a Blended Wing Body Aircraft—A Case Study*; Advances in Industrial Control; Springer: Berlin/Heidelberg, Germany, 2015.
22. Peigin, S.; Epstein, B. Computational fluid dynamics driven optimization of blended wing body aircraft. *AIAA J.* **2006**, *44*, 2736–2745. [CrossRef]
23. Campos, L.M.B.C.; Marques, J.M.G. On the minimization of the cruise drag due to pitch trim. In Proceedings of the 5th Council of European Aerospace Societies (CEAS) Air and Space Conference, Challenges in European Aerospace, Delft, The Netherlands, 7–11 September 2015; p. 87.
24. Rahman, N.U.; Whidborne, J.F. Propulsion and flight controls integration for a blended-wing-body transport aircraft. *J. Aircr.* **2010**, *47*, 895–903. [CrossRef]
25. Peifeng, L.; Binqian, Z.; Yingchun, C.; Changsheng, Y.; Yu, L. Aerodynamic design methodology for a blended wing body transport. *Chin. J. Aeronaut.* **2012**, *25*, 508–516.
26. Wildschek, A.; Stroscher, F.; Hanis, T.; Belschner, T. Fuel management system for cruise performance optimization on a large blended wing body airliner. *Prog. Flight Dyn. GNC Avion.* **2013**, *6*, 651–670.
27. Wildschek, A.; Bartosiewicz, Z.; Mozyrska, D. A multi-input multi-output adaptive feed-forward controller for vibration alleviation on a large blended wing body airliner. *J. Sound Vib.* **2014**, *333*, 3859–3880. [CrossRef]
28. Kumar, P.; Khalid, A. Blended Wing Body Propulsion System Design. *Int. J. Aviat. Aeronaut. Aerosp.* **2017**, *4*, 6.
29. Ammar, S.; Legros, C.; Trépanier, J.-Y. Conceptual design, performance and stability analysis of a 200 passengers Blended Wing Body aircraft. *Aerosp. Sci. Technol.* **2017**, *71*, 325–336. [CrossRef]
30. Panagiotou, P.; Fotiadis-Karras, S.; Yakinthos, K. Conceptual design of a Blended Wing Body MALE UAV. *Aerosp. Sci. Technol.* **2018**, *73*, 32–47. [CrossRef]
31. Campos, L.M.B.C.; Marques, J.M.G. On the maximisation of control power in low-speed flight. *Aeronaut. J.* **2019**, *213*, 1099–1121. [CrossRef]
32. Kim, H.; Liou, M.F. Flow simulation and drag decomposition study of N3-X hybrid wing-body configuration. *Aerosp. Sci. Technol.* **2019**, *85*, 24–39. [CrossRef]
33. Khan, T. Design and CFD Analysis of a Blended Wing UAV (A Conceptual Design). *J. Aerosp. Eng. Mech.* **2019**, *3*, 156–160.
34. Campos, L.M.B.C.; Marques, J.M.G. On the Handling Qualities of Two Flying Wing Aircraft Configurations. *Aerospace* **2021**, *8*, 77. [CrossRef]
35. Wang, G.; Zhang, M.; Tao, Y.; Li, J.; Li, D.; Zhang, Y.; Zhang, B. Research on analytical scaling method and scale effects for subscale flight test of blended wing body civil aircraft. *Aerosp. Sci. Technol.* **2020**, *106*, 106114. [CrossRef]
36. Footohi, P.; Bouskela, A.; Shkarayev, S. Aerodynamic Characteristics of the Blended-Wing-Body VTOL UAV. *J. Aerosp. Eng. Mech.* **2020**, *4*, 187–300.
37. Humphreys-Jennings, C.; Lappas, I.; Sovar, D.M. Conceptual Design, Flying, and Handling Qualities Assessment of a Blended Wing Body (BWB) Aircraft by Using an Engineering Flight Simulator. *Aerospace* **2020**, *7*, 51. [CrossRef]
38. Campos, L.M.B.C.; Marques, J.M.G. On a Method of Lagrange Multipliers for Cruise Drag Minimization. *J. Aerosp. Eng. Mech.* **2021**, *5*, 348–366.
39. Campos, L.M.B.C.; Marques, J.M.G. On the Comparison of Ten Pitch Trim Strategies for Cruise Drag Minimization. *J. Aerosp. Eng. Mech.* **2021**, *5*, 367–391.
40. Jemitola, P.; Okonkwo, P. Review of Structural Issues in the Design of a Box Wing Aircraft. *J. Aerosp. Eng. Mech.* **2019**, *3*, 161–166.
41. Kalinowski, M. Aero-Structural Optimization of Joined-Wing Aircraft. *Trans. Aerosp. Res.* **2017**, *4*, 48–63. [CrossRef]
42. Huijts, C.; Voskuijl, M. The impact of control allocation on trim drag of blended wing body aircraft. *Aerosp. Sci. Technol.* **2015**, *46*, 72–81. [CrossRef]
43. Valasek, J.; Harris, J. Derived Angle of Attack and Sideslip Angle Characterization for General Aviation. *J. Guid. Control. Dyn.* **2020**, *43*, 1039–1055. [CrossRef]
44. Lerro, A.; Brandl, A.; Gili, P. Model-Free Scheme for Angle-of-Attack and Angle-of-Sideslip Estimation. *J. Guid. Control. Dyn.* **2021**, *44*, 595–600. [CrossRef]
45. Milne-Thomson, L.M. *Theoretical Aerodynamics*; Dover Publications: New York, NY, USA, 1958.
46. Campos, L.M.B.C. *Complex Analysis with Applications to Flows and Fields*; CRC Press: Boca Raton, FL, USA, 2011.
47. Lamb, H. *Hydrodynamics*; Cambridge University Press: Cambridge, UK, 1931.
48. Campos, L.M.B.C. *Transcendental Representations with Applications to Solids and Fluids*; CRC Press: Boca Raton, FL, USA, 2012.
49. Landau, L.D.; Lifshitz, E.M. *Fluid Mechanics*; Pergamon Press: New York, NY, USA, 1953.
50. Campos, L.M.B.C.; Vilela, L.A.R. *Compressible Flow with Applications to Engines, Shocks and Nozzles*; CRC Press: Boca Raton, FL, USA, 2022.

51. NEFA (New Empennage For Aircraft) Project. Available online: https://cordis.europa.eu/project/id/G4RD-CT-2002-00864 (accessed on 12 February 2022).
52. Carrier, G.; Gebhardt, L. A Joint DLR-ONERA Contribution to CFD-Based Investigations of Unconventional Empennages for Future Civil Transport Aircraft. Available online: https://elib.dlr.de/21204/1/KATnet-CEAS_Paper25_Carrier_Gebhardt.pdf (accessed on 12 February 2022).